THE TENSILE DEFORMATION OF PURE VANADIUM SINGLE CRYSTALS AT LOW TEMPERATURES

by

ROBERT FORRESTER SNOWBALL

A THESIS SUBMITTED IN PARTIAL FULFILMENT
OF THE REQUIREMENTS FOR THE DEGREE OF
MASTER OF APPLIED SCIENCE
in the Department of
MINING AND METALLURGY

We accept this thesis as conforming to the standard required from candidates for the degree of MASTER OF APPLIED SCIENCE

Members of the Department of
Mining and Metallurgy

THE UNIVERSITY OF BRITISH COLUMBIA

October 1960

In presenting this thesis in partial fulfilment of the requirements for an advanced degree at the University of British Columbia, I agree that the Library shall make it freely available for reference and study. I further agree that permission for extensive copying of this thesis for scholarly purposes may be granted by the Head of my Department or by his representatives. It is understood that copying or publication of this thesis for financial gain shall not be allowed without my written permission.

Department of Mining and Metallurgy

The University of British Columbia,
Vancouver 8, Canada.

Date November 14th, 1960

ABSTRACT

An investigation of the low temperature tensile properties of vanadium single cyrstals was carried out, using zone-refined metal.

Single crystals of predetermined axial [110] orientation were grown by a melt solidification technique, using an electron beam, floating-zone refiner. Tensile specimens were prepared from these single crystals.

A plot of yield stress versus test temperature was found to be discontinuous and consisted of two curves which intersected at -125° C. The plot of log yield stress versus reciprocal temperature yielded two straight lines which also intersected at -125° C.

The slip system was identified as $\langle 111 \rangle \{112\}$, which is different from that found for iron single crystals.

X-ray, metallographic and electrical resistance data indicate that the phenomenon is primarily a yield point effect. The results of tensile tests performed on single crystals at a very low strain rate, and on polycrystalline specimens indicated that the temperature dependence of yield stress is itself orientation dependent.

Three possible explanations of the unusual temperature dependence of yield stress are given:

(1) A change in deformation mechanism occurs, for example, from slip to twinning.

(2) A minor ordering reaction occurs.

(3) A change in the mechanism by which dislocations are unlocked from their atmospheres occurs; for example, two impurity atmospheres surrounding different dislocations, each impurity showing a separate temperature dependence of yield stress.

ACKNOWLEDGMENT

The author wishes to thank Dr. J.A. Lund and Professor W.M. Armstrong for their supervision and encouragement, and Mr. R.G. Butters for his technical assistance during this investigation.

The author is also indebted to Dr. E. Teghtsoonian and R.W. Fraser for many helpful discussions.

The work was financed by the Defence Research Board, under D.R.B. Grant 7510-36, 'The Effect of Strain Rate and Temperature on the Deformation Behaviour of Body-Centered-Cubic Metals.'

TABLE OF CONTENTS

No.	FIGURES	Page

TABLES

THE TENSILE DEFORMATION OF PURE VANADIUM SINGLE CRYSTALS AT LOW TEMPERATURES

I. INTRODUCTION

The increasing demand for materials suitable for extreme elevated temperature service has directed investigators to many new fields in recent years. Exhaustive studies of ferrous and non-ferrous alloy systems have been made, yielding materials which fall far short of the stringent requirements of the high temperature field. More recently, the fields of ceramics, cermets and refractory metals have come into the foreground. Although preliminary results are very encouraging, these fields are still in infancy, and a great deal of fundamental work is required before a clear understanding of the behaviour of these materials is achieved. This investigation is part of a programme concerning the behaviour of refractory metals. More specifically, it is a fundamental study of the tensile properties of vanadium metal.

Vanadium metal has been an article of commerce for several years[1], used principally as a ferrous and non-ferrous alloying addition. Two serious limitations prevent its extensive use as a refractory base metal: it has a low melting point (1900 $\pm$ 25°C) relative to many other refractory metals and, more serious, the oxide which forms on the surface of vanadium and ductile vanadium-base alloys has a melting point of 675°C. It is still, however, a metal of interest because of its relatively low density (6.1 /cc), its high electrical resistivity, its good chemical corrosion resistance, its relatively high hot strength at intermediate temperatures up to 500°C, and its relative abundance.[3,4]

A survey of the literature indicates that, despite the interest in vanadium, surprisingly little is known of its physical metallurgy.

The objectives of this work were to study the temperature dependence of the tensile properties, and ductile-to-brittle transition behaviour of high purity vanadium single crystals and polycrystalline metal. It was proposed to perform these tests at various strain rates, and independently to evaluate in this manner the effect of strain rate on the low temperature tensile properties of vanadium.

II. A REVIEW OF PREVIOUS WORK

The pronounced transition from ductile-to-brittle behaviour is most common in metals having the body-centered cubic structure, primarily because these metals exhibit a strong temperature and strain-rate dependence of yield strength.

The condition for the occurrence of brittle or cleavage failure is that the yield strength must exceed the cleavage fracture strength, a condition which may be brought about by lowering the temperature or increasing the strain rate.

Wessel[34] has reviewed the literature concerning the theoretical aspect of the ductile-to-brittle transition and has summarized it in the following manner.

Cottrell and Bilby[20] and Fisher[11] describe yielding as the breaking away of dislocations from atmospheres of impurity atoms, which it is believed tend to form as a result of the migration of interstitial and other impurity atoms to the vicinity of dislocations, and there to exert a 'locking' effect on such dislocations. This concept of yielding does not require any prior plastic deformation. Since pre-yield plastic strain does occur, the concept of catastrophic yielding resulting only from the breaking loose of ~~Frank~~ Frank-Read sources from pinning atmospheres cannot adequately explain the yield phenomena encountered in body-centered cubic metals.

It is believed that the pre-yield plastic strain is due to the breaking away of an appreciable number of dislocations prior to the elastic limit. These dislocations are subsequently piled up on grain boundaries, impurity atoms or other barriers.

At high temperatures, the yield point is the result of the piled up dislocations being released, and more dislocation sources breaking away from anchoring atmospheres, resulting in the cataclysmic release of dislocations which causes the load to drop and results in the familiar upper and lower yield points.

At low temperatures, the stress level just prior to yielding is very high, and, because of the increased resistance to plastic deformation, higher localized stresses are required to enable piled-up dislocations to break through or away from barriers. As a result, high localized stresses can exist in front of piled up dislocations. These stresses can, in fact, be so high that they exceed the cohesive strength of the metal, and result in microcracking. Where material is more favorably oriented for flow, the piled up dislocations can result in plastic deformation. During the subsequent abrupt yielding, the microcracks grow in size and number, and eventually a stable crack forms which will propagate and result in brittle failure.

The abruptness of the transition from a flow-producing yield to a crack-producing yield is dependent on the particular metal and its chemical and metallurgical condition.

In general, most body-centered cubic transition metals exhibit a higher tendency for sharp yielding at low temperatures. Among the metals which exhibit this phenomenon are vanadium, niobium, chromium, molybdenum, tungsten and iron. Tantalum has not shown brittle behaviour in tension as low as 4.2°K. There are large variations in transition temperatures encountered and many variables appear to have a large influence.

The most important information contained in the literature concerns the influence on properties of the intrinsic contents of the im-

purity elements; hydrogen, nitrogen, carbon and oxygen. A limited amount of published data exists concerning the individual effects of these impurities, with the exception of hydrogen, for which more data is available,[5,9].

The term 'interstitial ~~impurites~~ impurities' will be applied to hydrogen, nitrogen, carbon and oxygen in the text which follows, although it is recognized that oxygen is normally a substitutional impurity.

A considerable volume of results based on studies of the tensile and impact properties of vanadium is now available in the literature, although the results are contradictory and inconclusive in some cases. This is due largely to the fact that the materials used in each case were of different purities, and the results cannot, therefore, be compared on a rigorous basis.

All previous investigations with the exception of the work by Loomis and Carlson[9] were carried out using a commercial or sub-commercial grade of metal, and one paper[5] reported the effect of contaminating commercial vanadium with hydrogen. Typical analyses of material used by previous workers is given in Table I. It is clear from the foregoing discussion that the purity of the metal must be known if the results are to be of value.

TABLE I

TYPICAL IMPURITY CONTENT OF VANADIUM METAL USED BY OTHER INVESTIGATORS

Ref.	Type	C(wt%)	N(wt%)	O(wt%)	H(wt%)	Fe	Si	Ca	Al	W	Ref.
3	Arc Melted	0.09	0.07	0.057	0.0004	0.005	0.005			0.02	3
4	Bomb-Reduced	.03-.07	.02-.04	.05-.12	.001-.004						4
5	Bomb-Reduced	0.2	0.01	0.02	0.003	0.015	0.01	0.02			5
7	Bomb-Red-Extruded	.13	.009	.03	.002	0.2	0.05	0.1	0.1		7
8	Bomb-Reduced	.036-.047	.047-.083	.030-.070	.0028-.0059						8
9	Bomb-Reduced	.08	.02	.02	.006	0.02	0.02	0.02			9
9	Crystal Bar	.024	.005	.01	.001	0.02	0.02	0.02			9
10	Arc Cast	.029-.094	.032-.060	.043-.110	.001-.004						10

The tensile properties of vanadium, in common with other body-centered cubic transition metals are sensitive to a number of factors, including the interstitial content of the metal, the type and alignment of the specimen in a tension test, the strain rate and the type of testing machine used. In general, an increase in the interstitial content or strain rate increases the yield strength of the metal. A 'soft' tensile machine, such as a heavy hydraulic unit tends to give a lower value of yield strength,[10] since the upper yield point may be suppressed by the internal motion of the machine. A 'hard' machine such as one having a screw-driven cross-head does not tend to suppress yielding phenomena. The other major factor involved is the alignment of the specimen.[10] Misalignment, which is more difficult to avoid with sheet specimens than cylindrical, shouldered specimens, will also cause suppression of the yield phenomenon. For these reasons, probably less significance should be attached to strength values reported which are based on data obtained from soft machines using sheet specimens or where no particular attention was paid to specimen alignment through the use of a universal-type of gripping mechanism. This applies especially to investigators who used standard bomb-reduced vanadium of normal impurity content, and reported considerable ductility with no heterogeneous yielding phenomenon.[1,8]

Previous investigations of the variation of tensile properties of vanadium with temperature in the range between 25°C and -196°C have yielded contradictory results which may be roughly divided into three categories: (1) Those showing no abnormal behaviour,[3,8,10] (2) those showing abnormal temperature dependence of yielding,[9] and (3) those showing abnormal ductility behaviour.[5,6,9]

Considering the first group, Pugh[3] studied the tensile properties of sheet specimens for constant strain rate and at temperatures between 78° and 1500°K. Specimens were cut from arc-melted, rolled and annealed metal, of the purity indicated in Table I. Evaluation was made in terms of ultimate tensile strength, 0.2 percent yield strength, strain hardening and rate sensitivity of the flow stress. He concluded that vanadium has a temperature dependence of tensile properties which is characteristic of body-centered-cubic metals, with the following features: (1) a high temperature sensitivity at low temperatures, (2) the occurrence of discontinuous yielding at low and intermediate temperatures, and the appearance of minima in strain rate sensitivity and elongation, and maxima in strain hardening and strength relationship at about 700°K, indicating strain aging behaviour. Clough and Pavlovic[8] studied the flow, fracture and twinning of commercially pure vanadium. They performed tensile tests in the temperature range from 200° to -196°C, and V-notch Charpy tests in the temperature range 150° to -100°C. Bomb-reduced metal, of the purity indicated in Table I was used. Tensile tests, made from round, threaded-end specimens exhibited a five-fold increase in yield strength (using a 0.2 percent offset), a three-fold increase in ultimate tensile strength, and a ductile-to-brittle transition over this range of temperature, as shown in Figure 1. The variation of yield strength was correlated to Fisher's application of the Cottrell-Bilby theory of yielding.[11] It should be noted that Clough and Pavlovic used a hydraulic tensile machine, and any heterogeneous yielding phenomena were probably obscured. Charpy tests indicated that both $\{100\}$ and $\{110\}$ are active cleavage habit planes. Mechanical twins were formed by impact loading at test temperatures of -78°C and lower. These twins were found to occur on $\{112\}$ planes, apparently only within one or two grains of a cleaved surface.

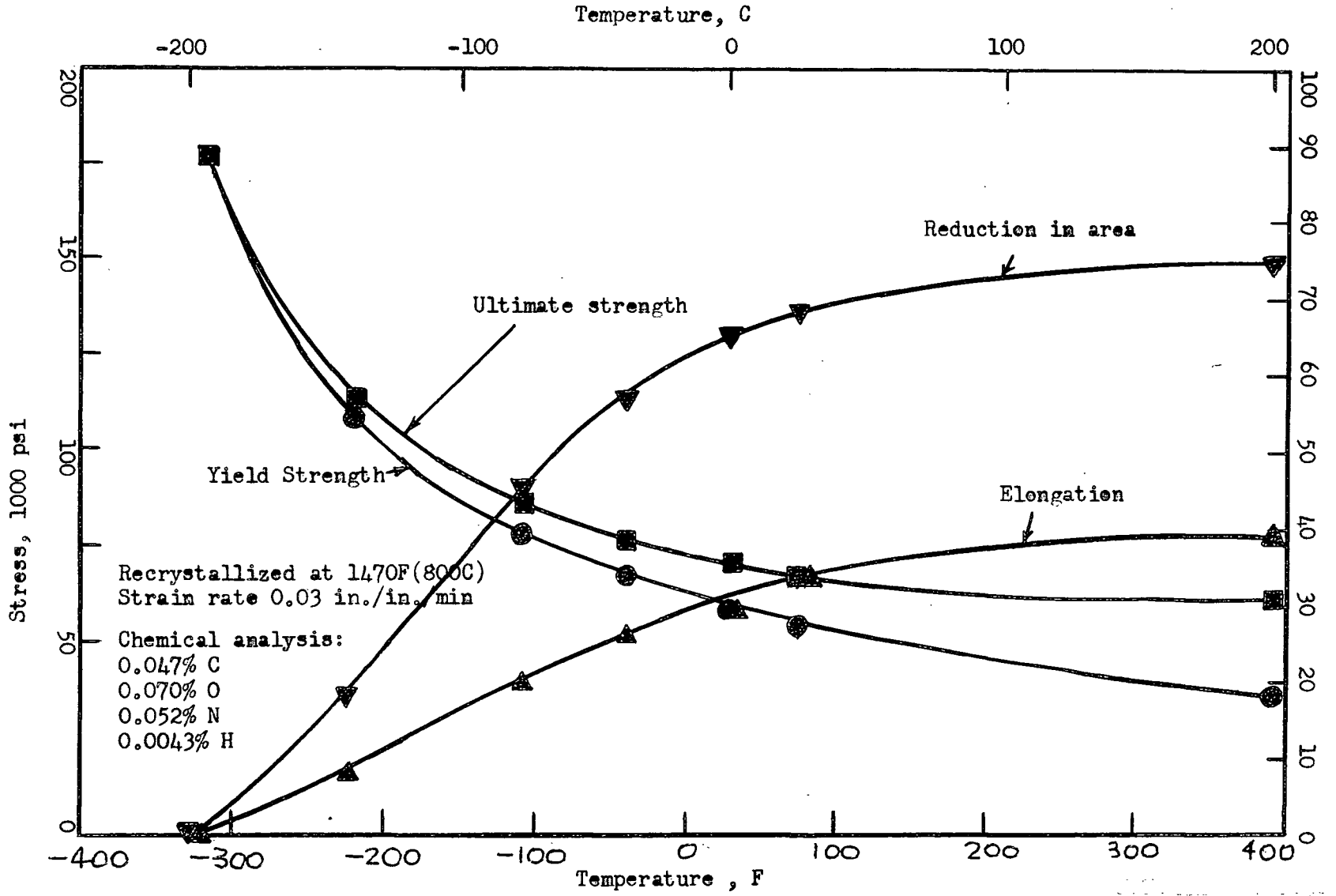

Figure 1. Temperature dependence of the Tensile Properties of Vanadium From Clough and Pavlovic

Farrell has recently published a paper[10] concerning the properties of unalloyed vanadium consolidated by vacuum consumable-electrode arc melting, hot extrusion and cold working. The results presented include short-time tensile properties for bar and sheet in the temperature range from 1100° to -196°C, yield point and strain aging phenomena, notched-bar tensile properties, true stress-true strain curves, the strain hardening coefficient and exponent, elastic modulus, work-hardening characteristics, bend and Erichsen test data, and crystal orientations determined by X-Ray studies.

The results of Farrell's tensile tests are of wide interest, particularly with regard to yield-point phenomena. Almost all tests were performed using a Baldwin-Lima-Hamilton Universal Testing machine. Load-elongation curves were recorded autographically. In all cases, fully annealed ~~cylindrie~~ cylindrical specimens displayed distinct upper and lower yield points, whereas sheet tensile specimens which had been given identical cold working and annealing treatment showed no evidence of similar behaviour. The lack of a distinct yield point for sheet specimens was considered to be due to (a) load eccentricity and/or (b) the use of a 'soft' hydraulic tensile machine. To resolve this problem the following tests were made:

Sheet specimens of identical preparation were tested in a 'soft' (hydraulic) machine and a 'hard' (Instron screw-driven) machine. The curves from the soft machine showed no yield phenomena, whereas the curves from the 'hard' machine showed distinct upper and lower yield points. Specimens were then prestrained in the 'soft' machine to 3 percent elongation to remove any eccentricity that may have existed. To relieve the stresses introduced by prestraining, the specimens were annealed in the

machine, under a load of 1000 to 2000 pounds per square inch. Subsequent testing showed distinct, though slight, yield phenomena. It may therefore be assumed that suppression of yield phenomena may be caused both by load eccentricity and the use of a 'soft' machine.

Consider now the second group of investigations (i.e. those showing abnormal temperature dependence of yielding). Loomis and Carlson[9] studied the tensile properties of vanadium between room temperature and -196°C. The materials used were bomb reduced and crystal bar metal, of the purities indicated in Table I. Figures 2 and 3 illustrate the data of Loomis and Carlson; Figure 2 for bomb-reduced metal, and Figure 3 for crystal-bar metal. No explanation was given for the rapid increase in yield strength encountered at -80°C for bomb-reduced metal and at -100°C for crystal bar metal. Further discussion of this paper will appear later in the present thesis with regard to the anomalous ductility behaviour encountered.

A consideration of the third group of investigations (i.e. those showing abnormal ductility behaviour) shows that three independent investigators[5,6,9] found a ductile-brittle-ductile transition, that is, a ductility minimum. Roberts and Rogers[5] used cylindrical wire specimens and foil specimens of the nominal purity shown in Table I. After hydrogenation to 0.042, 0.062 and 0.045 weight percent hydrogen, the specimens were tested in tension. The reduction in area of the hydrogenated cylindrical specimens showed a minimum at approximately room temperature. Unhydrogenated vanadium showed no sharp ductility change to -196°C. The mechanism whereby hydrogen causes this phenomenon, according to Roberts and Rogers,[5] is not as yet understood. Magnusson and Baldwin[6,13] evaluated the effect of strain rate on the ductility minimum at a hydrogen content of 80 parts per million, and reported that at high strain rates (19000 in/in/min) no minimum is encountered, and at liquid nitrogen temperatures the metal

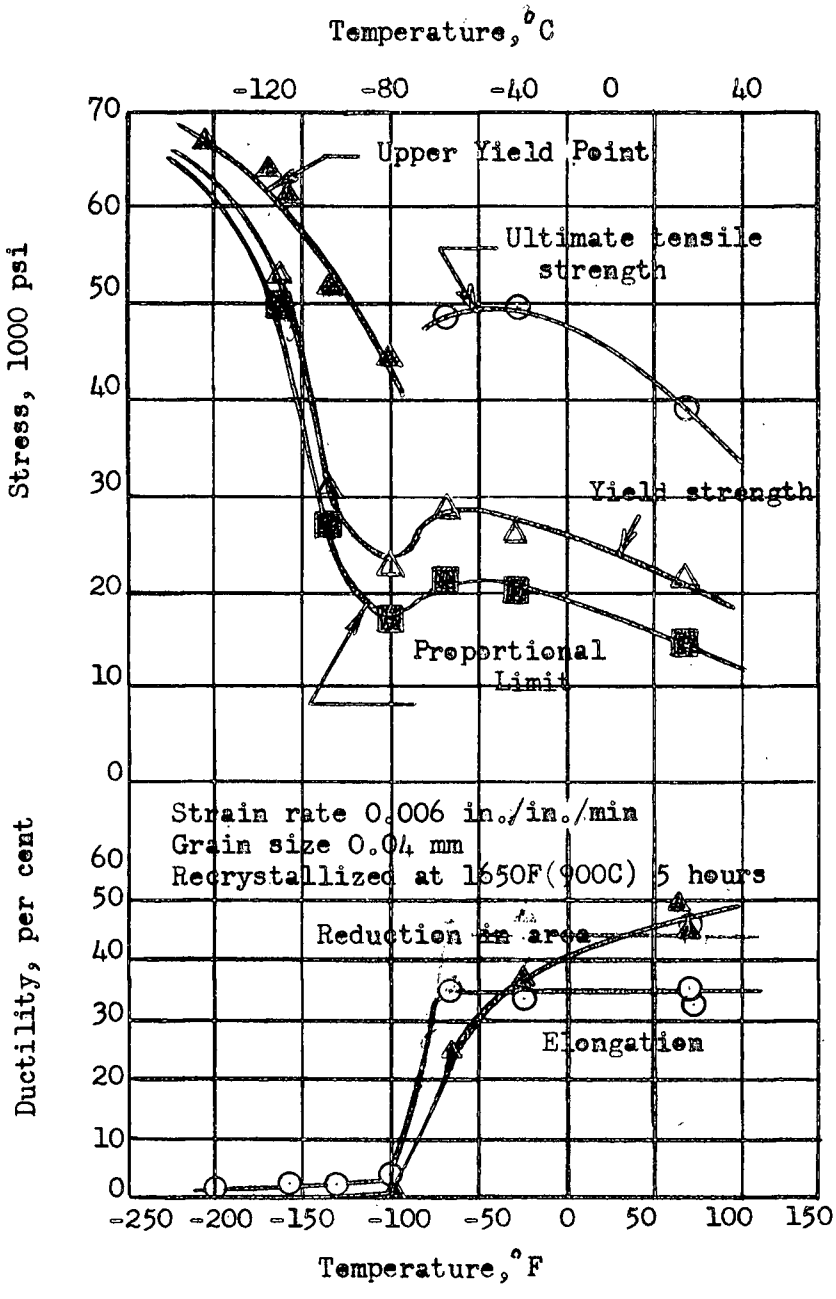

Figure 2. Tensile properties of bomb-reduced vanadium at low temperatures, after Loomis and Carlson[9]

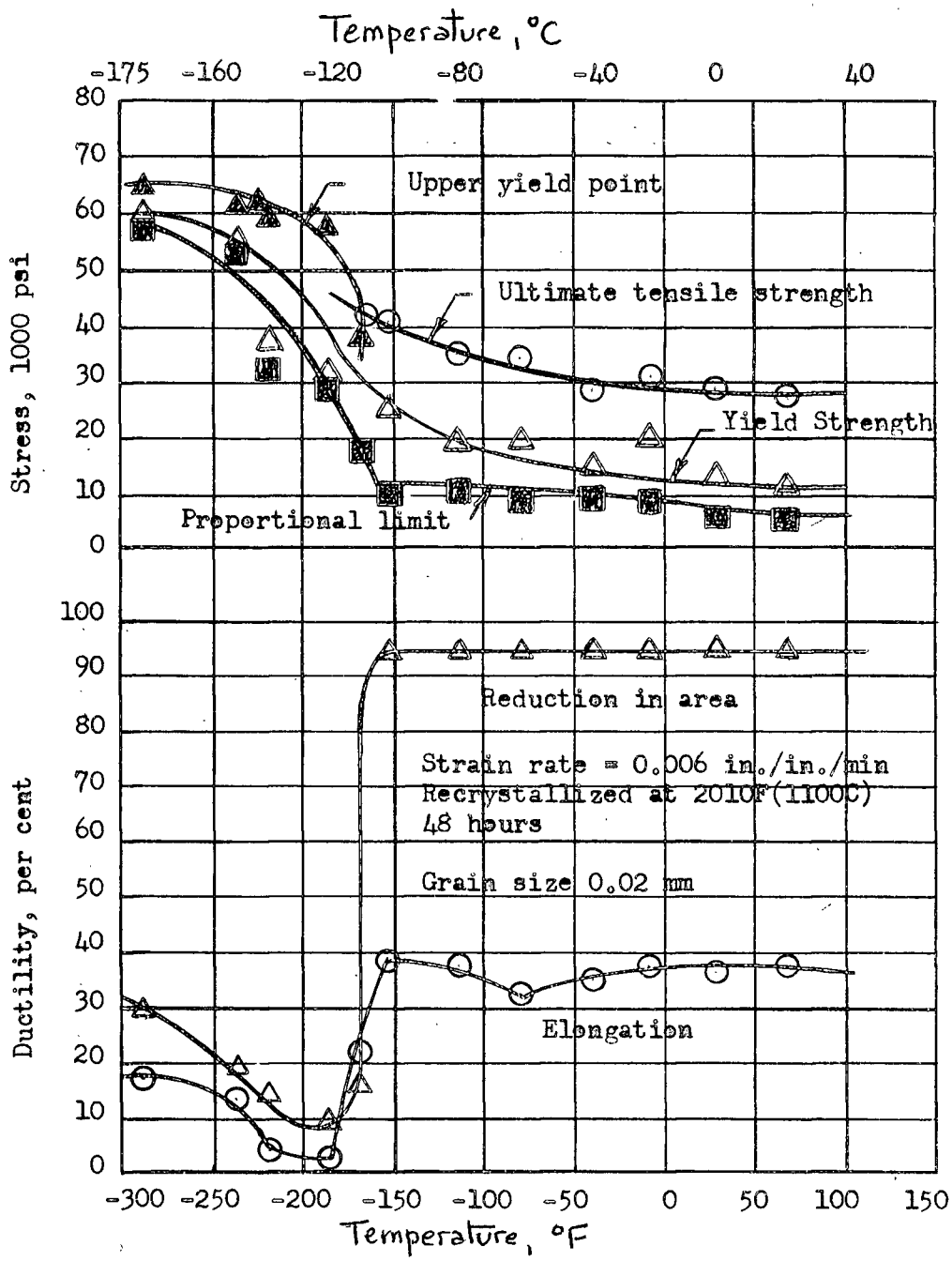

Figure 3. Tensile properties of crystal-bar vanadium at low temperatures after Loomis and Carlson[9]

sustains more than 30 percent reduction in area before fracture. At low strain rates (0.05 in/in/min), they report a ductility minimum at about -100°C, with a subsequent recovery of the reduction in area to a value of 15 per cent at -196°C. The results of these investigations[5,6] are considered by some to indicate that the low temperature brittleness of vanadium may be associated with hydrogen embrittlement, rather than ductile-to-brittle transition behaviour.[13]

Loomis and Carlson[9] found a progressive decrease in reduction in area from room temperature to -70°C, and a fairly sharp transition of the elongation curve between -60° and -70°C for bomb-reduced metal (Figure 2). With crystal bar vanadium they found a sharp transition from ductile-to-brittle behaviour for both elongation and reduction in area values between -100° and -120°C. They also found a ductility minimum for crystal-bar vanadium at temperatures of -150° and -180°C. A comparison of the ductility curves for the bomb-reduced and crystal-bar vanadium of Loomis and Carlson also gives a qualitative idea of the effect of purity on the transition temperature.

Bend test data on bomb-reduced metal obtained by Loomis and Carlson[9] showed a sharp transition from ductile-to-brittle behaviour at -60° to -70°C, in good agreement with the tensile data discussed earlier. At low temperature a slight increase in ductility was observed, although not so pronounced as that observed for tension tests of the crystal bar metal. Loomis and Carlson also used bend tests to evaluate the effect of interstitials on the transition temperature. Figure 4 illustrates these results. Bend tests on the higher purity crystal bar material showed that the transition was below -150°C.

From the foregoing discussion, it is evident that the cause of the ductility change found in vanadium (and other body-centered-cubic metals),

and the effect that impurities, testing temperature and grain boundaries have on it are not clearly understood. Tensile tests at temperatures between room temperature and -196°C are rather exiguous and the results of different investigators are not in good agreement. Also, apparently no investigation has been carried out previously using single crystals of vanadium.

Of the work reviewed in this paper, only that of Loomis and Carlson[9] and that of Clough and Pavlovic[8] is of use as a basis of reference in the present study. In all other cases mentioned[1,3,5-7,10,12] either the range of temperature studied was above room temperature[2] or the data were not sufficiently detailed between room temperature and -196°C.

Further reviews of previous work used in the analysis of the data obtained in the present work will be made in the appropriate section of the thesis.

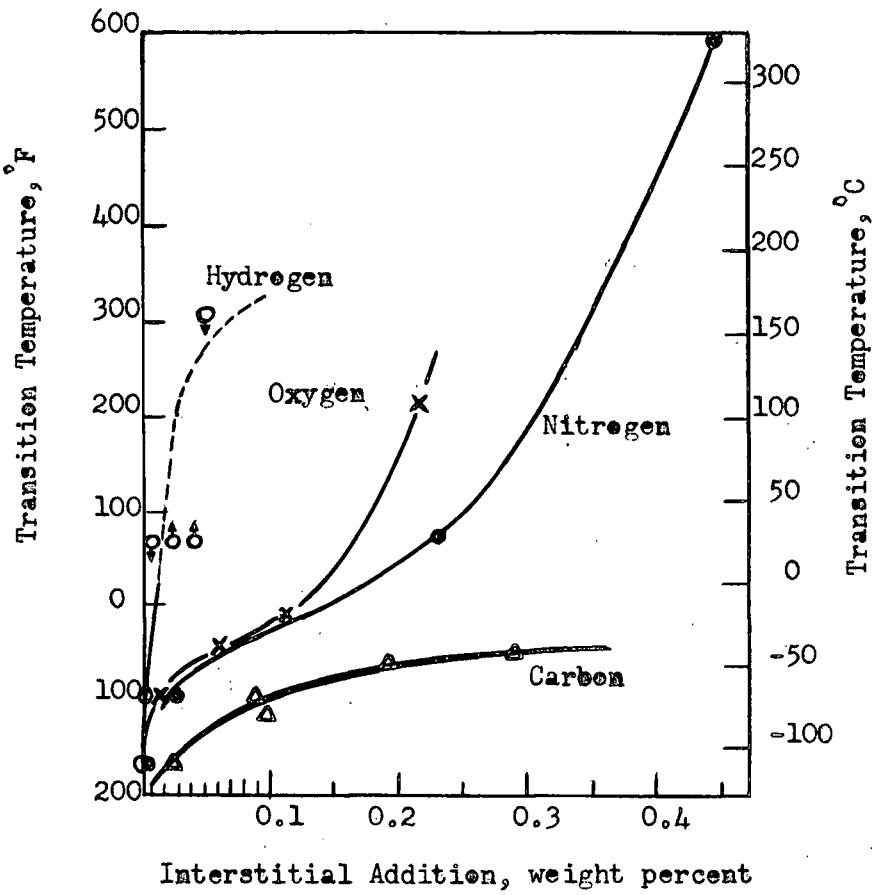

Figure 4. Effect of interstitial impurities on the ductile-to-brittle transition of bomb-reduced vanadium, after Loomis and Carlson[9]

III. EXPERIMENTAL

A. MATERIALS

The vanadium used in this investigation was supplied by Union Carbide Metals Company and was prepared by the bomb reduction of V_2O_5 by calcium[2]. The as-received material was analysed for interstitial impurities, with the results shown in Table II.

TABLE II

ANALYSIS OF AS-RECEIVED VANADIUM

Element	Wt%
C	0.0275
N	0.0048
O	0.0510
H	0.00032

The as-received metal was in the annealed condition, and metallographic examination showed the presence of a second phase which resembled in all characteristics a phase identified by Clough and Pavlovic[8] as V_2C.

The metal used in this investigation was taken entirely from one production batch, and was supplied in the form of 1/4-inch diameter rod.

B. PURIFICATION

Purification of the as-received metal was carried out in a vertical floating-zone electron bombardment unit similar to the one described by Calverly, Davis and Lever[14].

1. Construction of the Zone Refiner

The zone refiner was built entirely by the technical staff of the Department of Mining and Metallurgy of the University of British Columbia,

and the details of construction and assembly are shown in Figures 5 and 6.

(a) Power Supply

The power supply consists essentially of a 2300 volt d.c. power supply, with a current stabilizer. It supplies 2300 volts d.c. at 300 milliamps (i.e. 690 watts). The circuit details, as well as suggested modifications are given in Appendix II. A relay is incorporated to cut off the power in case of overload. The cathode is supplied from a transformer delivering up to 10 amps at 11 volts from a Variac-controlled mains input.

Automatic control of the power input is attained by emmission control, in which the bombardment current is kept constant by automatically adjusting the cathode temperature. Manual control of the power input is also possible, by direct connection to the cathode supply variac. Details of the control system are shown in Appendix II.

(b) Furnace

It is convenient to ground the specimen and to operate the cathode at a high negative potential, and the cathode leads and beam-forming plates must therefore be electrically insulated from each other and from the rest of the apparatus.

The electrode system is suspended inside a 2-foot long by 7-inch diameter pyrex tube, and is attached to the top plate by the main support rods (10, Figure 5). Movement of the specimen is facilitated by an O-Ring vacuum seal in the top plate, through which a central drive rod protrudes (2, Figure 5). The drive-rod is connected to the main crosshead (8) and specimen (1). The whole assembly is pulled upward by a motor-driven gearing

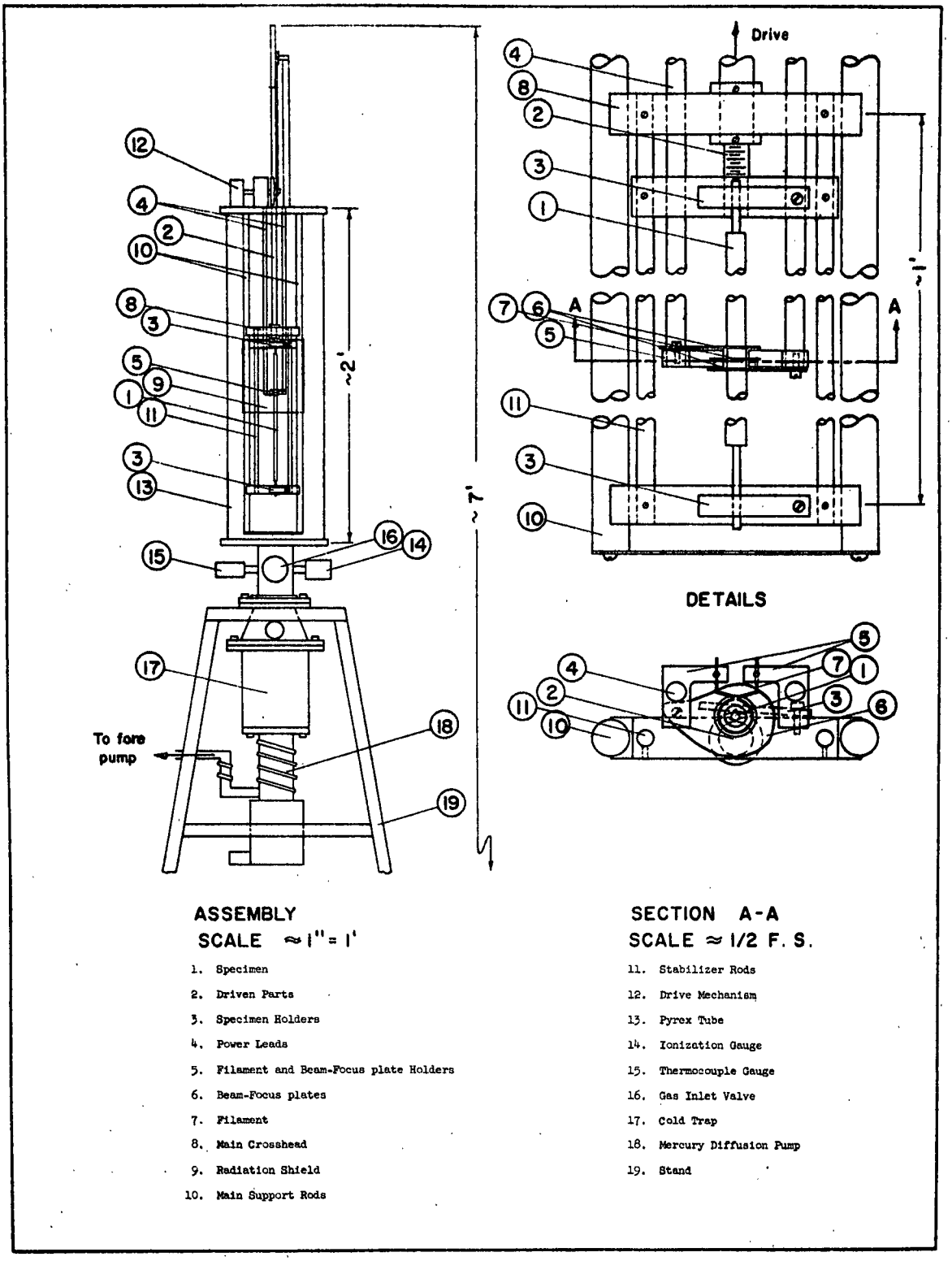

Figure 5. Construction of the Zone Refiner

Figure 6. Photograph of the Assembled Zone Refiner and Power Supply

arrangement (12) which allows travel speeds of 50, 25, 10, and 5 centimeters per hour.

The cathode or filament (7), the shape of which is shown in Section A-A, Figure 5, is made from 0.010 inch diameter tungsten wire, and is attached by screws to the filament and beam-focus plate holders (5, Figure 5). Connection of this type allows quick replacement of a broken filament. The purpose of the beam-focus plates (6) is to form a narrow zone, which is important if a uniform cross-section of the refined specimen is desired.

The heated zone of the furnace is surrounded by a molybdenum radiation shield (9) (Figures 5, 6,) to protect the glass and to reduce the radiation glare. Provision for viewing the specimen is made by mounting a glass microscope slide in the front of the radiation shield.

The specimen is rigidly attached to the crossheads by screw-clamp specimen holders (3). The specimen is mounted in two sections, so that no lateral forces exist in the specimen.

The furnace is also equipped with a gas inlet valve, and suitable gas pressure-measuring devices.

(c) Vacuum System

The vacuum system in this apparatus consists of an Edwards liquid nitrogen cold trap in series with an Edwards 35 liter per second, two stage mercury diffusion pump. This is connected to a Duo-Seal fore pump (rated at 50 liters per minute, free air capacity) by a one inch diameter high pressure hose. This system provides an operating vacuum of 10^{-5} millimeters of mercury, after only 15 to 20 minutes of pumping time.

2. Operation of the Zone Refiner

The specimen is mounted in two sections in the manner previously described so that fusion does not cause a lateral deflection of the specimen.

When the desired operating vacuum has been reached, the filament is heated to a high temperature and allowed to outgas for a period of ten to fifteen minutes. The high voltage is then turned on and the specimen is heated slowly, thereby allowing surface outgassing to take place. The two sections are then welded together. The specimen may then be zone-refined. Care must be exercised in choosing the correct voltage and current settings, so that a stable molten zone is assured. Because of the high

vapor pressure of vanadium at its melting point, it was necessary to open the system after each pass and remove layers of deposited metal from the radiation shields and beam-focus plates. It was also necessary to change the viewing glass regularly.

Each bar of vanadium, eight inches long, was given five zone-refining passes. The appearance of the metal after 5 passes was a reasonably smooth and very lustrous bar.

3. Purity of the Zone-Refined Metal

The purity of the zone-refined vanadium bars was substantially higher than that used by any previous investigator whose work is reported in the literature. The results of analysis on three bars appear in Table 3. For reference purposes, these analyses are compared to that of very high-purity crystal bar vanadium prepared by Carlson and Owen[30] using an iodide refining process. The two types of metal are of almost exactly the same total interstitial impurity content; the difference lies principally in carbon and nitrogen.

TABLE III

COMPARISON OF HIGH PURITY VANADIUM METAL

Specimen	Treatment	Wt. % Impurity			
		C	N	O	H
As Received	Bomb-reduced	0.0275	0.0048	0.0510	0.00032
V-16	Zone-Refined-5 passes	0.0066	0.0064	0.0090	0.00042
V-06	Zone-Refined-6 passes	0.0082	0.0089	0.0060	0.0028
V-13	Zone-Refined-6 passes	0.0056	0.0091	0.0050	0.0006
Ref. 30	Iodide Refined	0.015	0.0005	0.004	0.001

The zone-refined metal is also compared in Table III to the as-received material obtained for this investigation. The impurities most effectively

removed are carbon and oxygen, while nitrogen and hydrogen concentrations do not appear to be appreciably affected by zone refining.

C. SINGLE CRYSTAL GROWTH AND ORIENTATION

Single crystals were grown in the zone refiner, using a melt-solidification-zone-refining technique. Zone-refined bars were seeded with a vanadium single crystal rod whose axial direction was [110] . This crystal was obtained by preferential growth during the five-pass zone-refining process of one of the bars. After one pass, (giving the bars, effectively, six zone-refining passes) the crystal was examined by the Laue back-reflection X-Ray technique to be certain that the bar was, in fact, a single crystal over the whole length. Figure 7 shows five single crystals grown by the above technique, while Figures 8 and 9 show Laue pictures of one of the bars. Figure 8 was taken at the top end of the bar, and Figure 9 at the bottom end.

Figure 7. Photograph of Vanadium Single Crystals Grown by the Melt-Solidification-Zone-Refining Technique

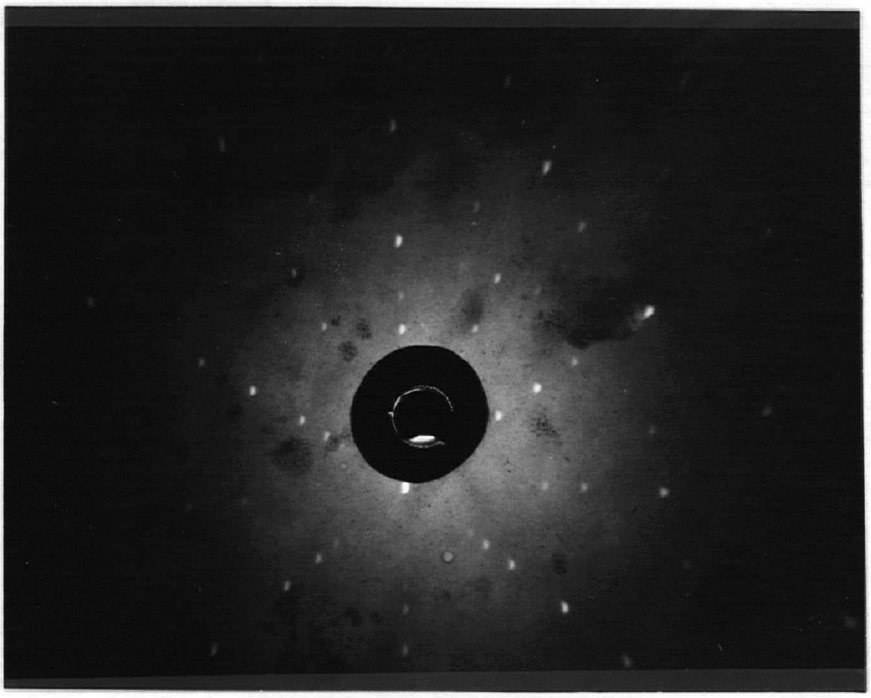

Figure 8. Laue Photograph near the top end of V-14

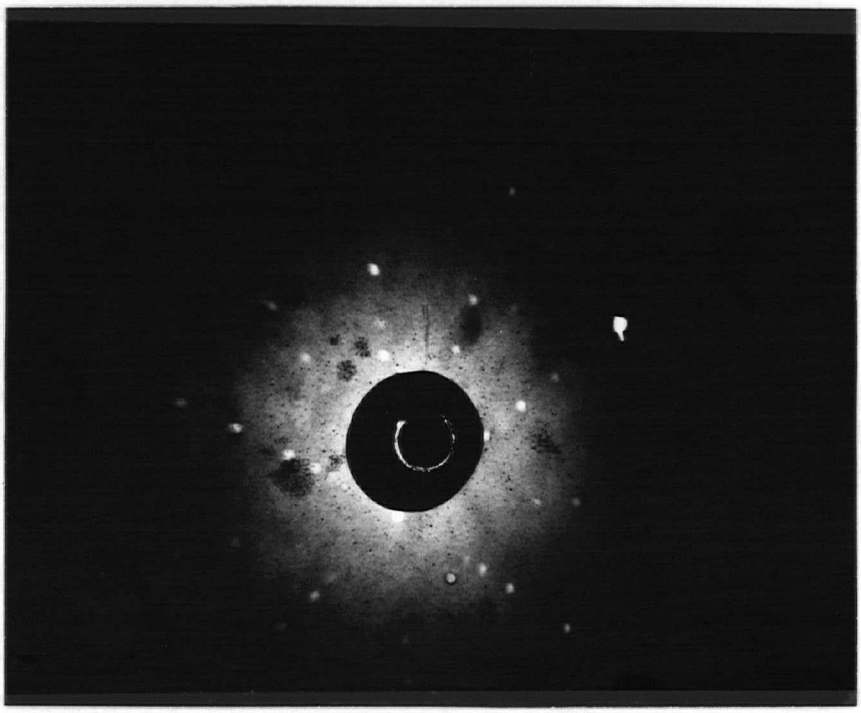

Figure 9. Laue photograph near the bottom end of V-14

D. SPECIMEN PREPARATION

1. Machining

The single crystal bars as shown in Figure 7 were cut into five equal lengths of approximately 1.25 inches using a jeweller's saw. The pieces were then mounted in a lathe and carefully machined to the shape of tensile specimens with a gauge section approximately 0.8 to 1 inch long and one-eighth inch in diameter. The maximum depth of cut taken in a single pass on the lathe was 0.003 inches. The machined specimens were then polished with 000 emery paper while mounted in the lathe.

2. Electropolishing

After machining, all specimens were electropolished for ten minutes, removing a layer of approximately 0.002 inches from the surface of the specimen. The solution used was a mixture of 40 cc of concentrated sulphuric acid, 160 cc of methyl alchohol and approximately 20 drops of water. A potential of 12.5 volts gave a current of 1.5 amps, and provided a very satisfactory surface finish.

3. X-Ray

Laue photographs of randomly selected specimens were taken to be sure that any effects of machining had been completely removed. A typical reproduction is shown in Figure 10.

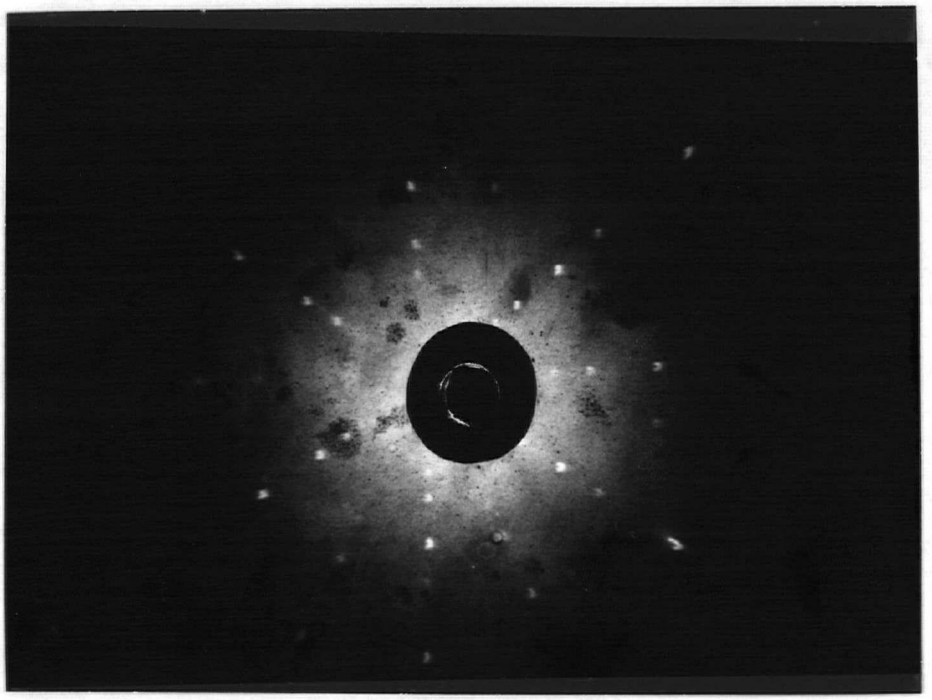

Figure 10. Laue Photograph of machined and electropolished tensile specimen.

4. Preparation of Polycrystalline Specimens

Two zone-refined bars were used to make ten polycrystalline specimens. After the bars had been cut into lengths, they were severely deformed by lateral compression in a hydraulic press. This treatment was followed by machining in a lathe, taking deep cuts and thereby encouraging further deformation. After the usual mechanical polishing in the lathe, the specimens were annealed at 900°C for four hours. The specimens were then electropolished, etched and examined metallographically, to be certain that complete recrystallization had occurred, and that the grain size was relatively uniform. Since only a semi-quantitative analysis of the tensile behaviour of these specimens was planned, no particular attention was paid to the actual grain size or the degree of preferred orientation. It is interesting to note that there was no evidence of the second phase (V_2C) mentioned earlier in this paper.

E. TESTING PROCEDURE

1. Gripping and Mounting of Test Specimens

The design of the grips used to hold tensile specimens in this work are shown in Figure 11. The grips were threaded into the mounting device as shown in Figure 12, which is a photograph of a mounted specimen, ready for testing. The mounting device was of a universal-type construction, equipped with roller bearings set at 90° to each other, thus ensuring uniaxial tensile loading of the specimens.

The mounting device was suspended from the lower (movable) crosshead of the tensile machine, with the upper jaw attached to the load cell by means of a long steel rod which projected through the crosshead (Figure 12). By using this method, the whole mechanism, plus an electrically driven stirrer, could be immersed in a Dewar flask containing the appropriate refrigerant. The flask was placed on a plywood shelf provided for that purpose (Figure 12).

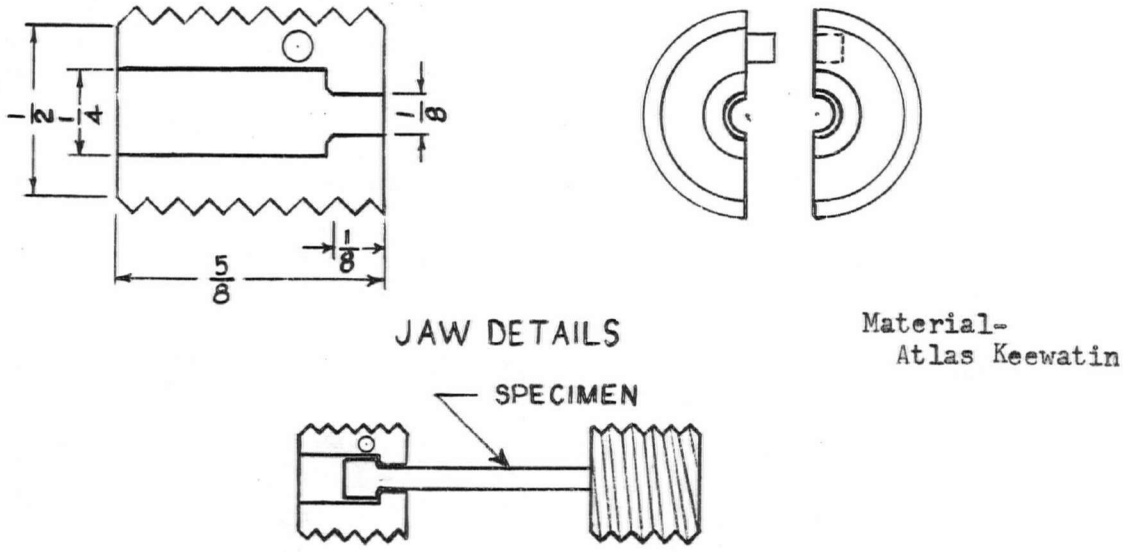

Figure 11. Jaws for Gripping Specimens

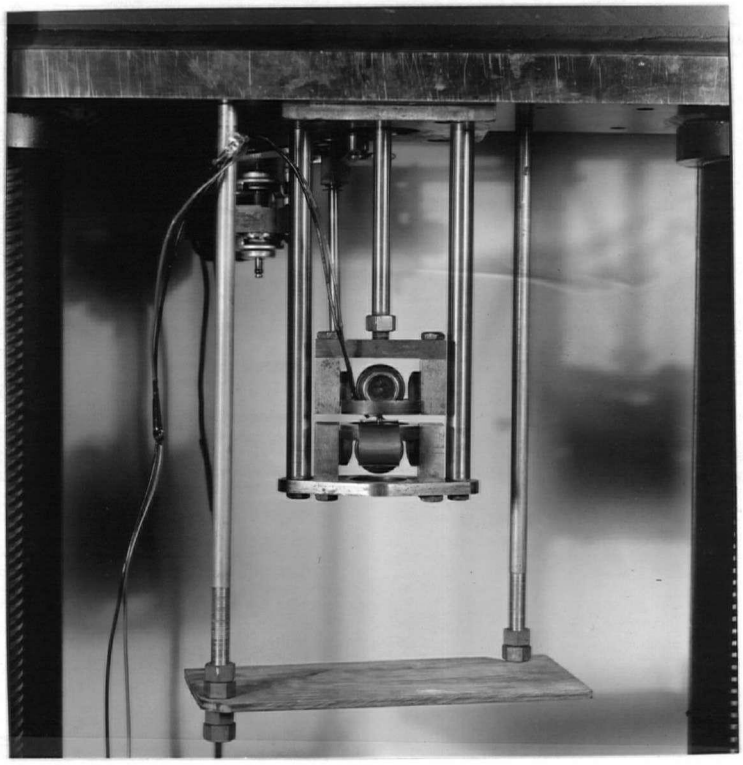

Figure 12. Photograph of mounted specimen, ready for tensile testing

2. Temperature Measurement

Temperatures were measured with a copper-constantan thermocouple which had been calibrated and found correct at room temperature and liquid nitrogen temperature. The thermocouple is rated by the manufacturer[15] as accurate to ± 2 per cent between -185° and -60°C, and ± 1-1/2 percent between -60°C and 100°C. The thermocouple was attached to the surface of all specimens by means of a fine wire.

3. Temperature Control

Test temperatures of -196° and -183°C were achieved by immersing the mounted specimens in a Dewar flask filled with liquid nitrogen and liquid oxygen, respectively.

Test temperatures between room temperature and -140°C were achieved by immersing the mounted specimens in a flask filled with petroleum ether, and cooled by a small, externally fed vessel filled with liquid nitrogen. Temperatures were measured at the start of the test, at the yield point and at the end of the test. The temperatures taken at the beginning and end of the test were only used to determine the total change over the length of the test.

Test temperatures between -183° and -140°C were achieved by submerging the mounted specimens in liquid nitrogen. When equilibrium had been reached the flask was removed, the nitrogen was poured out, and the empty flask was replaced. The apparatus and specimen were allowed to warm at a heating rate which was found by measurement to be 1°C per minute. Since tensile tests required about two to three minutes, the temperature variation was not more than ± 1.5 degrees. Again, the temperature taken at the yield point was used in subsequent calculations.

4. Test Procedure

The tensile machine used in this work was a 10,000 pound capacity Instron screw-driven unit, with the gripping mechanism modified as previously shown.

Mounted specimens were immersed in the coolant for a period of 10 to 15 minutes prior to testing.

All polycrystalline, and most single crystal specimens were tested at a crosshead speed of 0.05 inches per minute. Nine single crystal specimens were tested at a crosshead speed of 0.002 inches per minute.

All load-elongation curves were recorded autographically. Typical curves for various temperatures are shown in Figure 13.

Specimens after testing were carefully packaged and retained for subsequent metallographic and X-Ray examination. Typical broken specimens are shown in Figure 14.

The results of all tensile tests were calculated and tabulated and appear in Appendix I.

Specific procedures used in other parts of the experimental work are described in the appropriate section of the thesis.

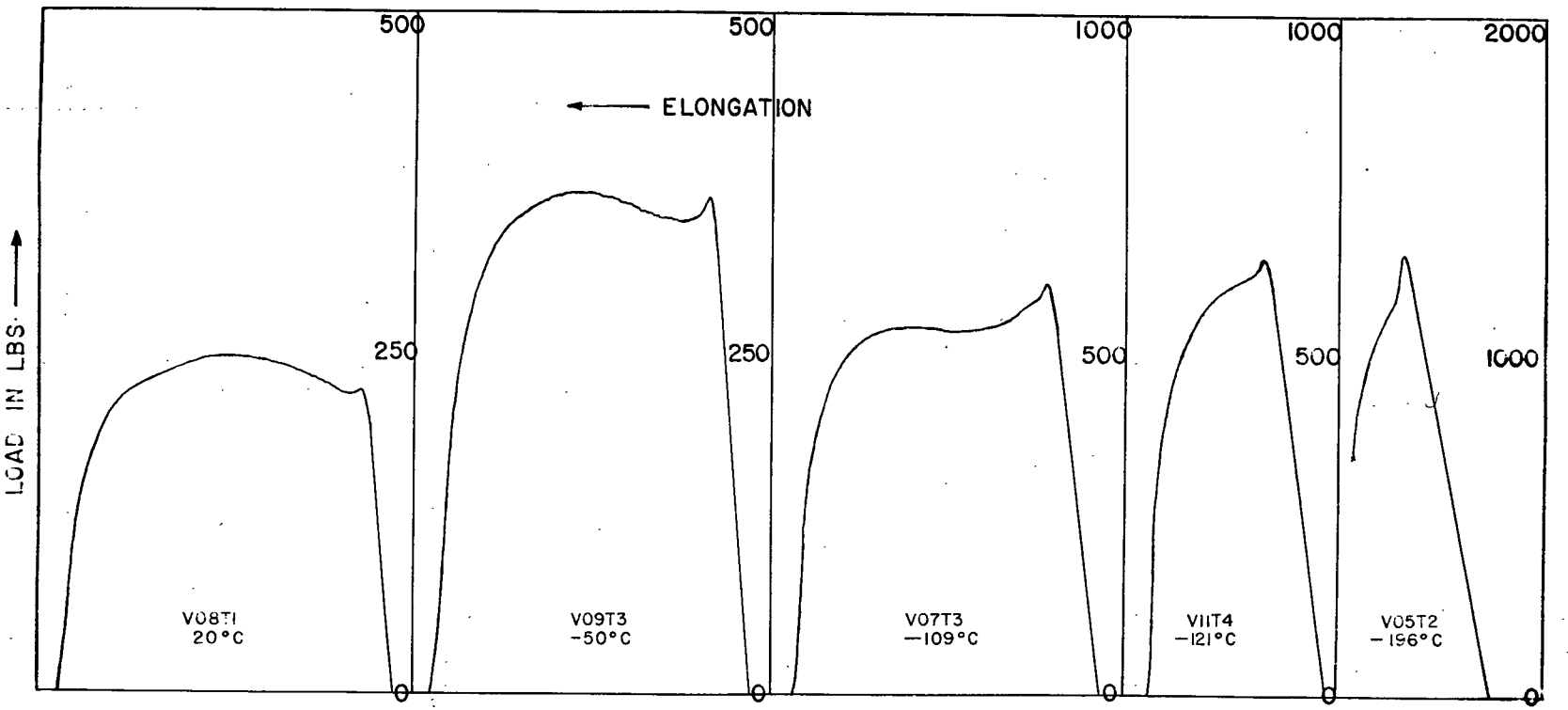

Figure 13. Typical Load-Elongation Curves at Different Temperatures

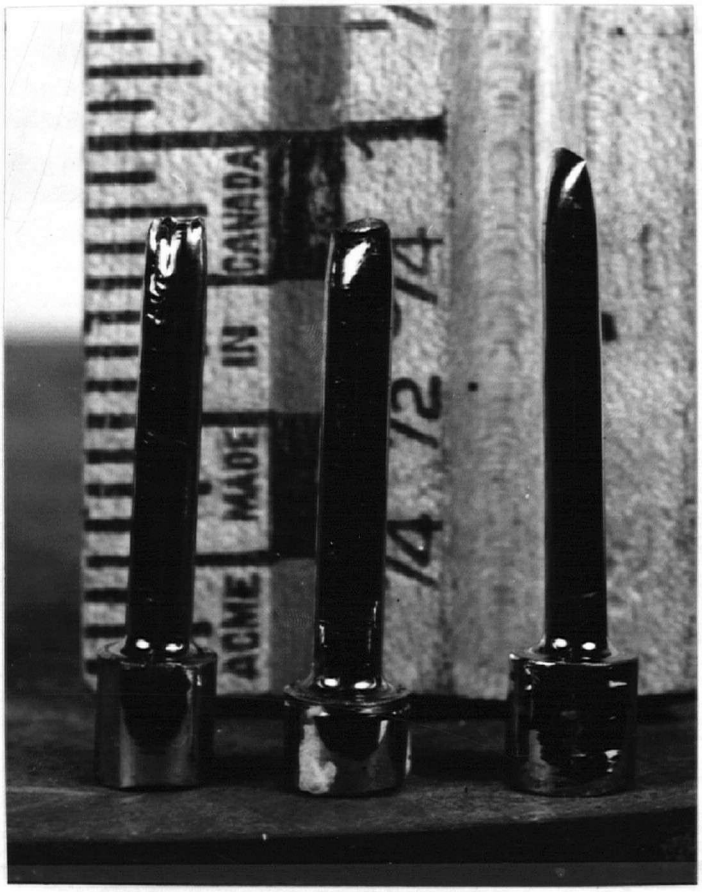

Figure 14. Typical broken specimens, Left to right:
polycrystalline specimen (-122.5°C)
single crystal (-196°C),
single crystal (24°C)

IV. EXPERIMENTAL RESULTS

A pronounced temperature dependence of the mechanical properties of the zone-refined vanadium was observed. The dependence of the yield stress, flow stress and percent elongation was determined over the temperature range from 25°C to -196°C.

A. SINGLE CRYSTALS - RATE OF STRAIN 0.055/min.

1. Yield Stress

Figure 15 shows the upper yield stress as a function of temperature. The plot of yield stress against temperature did not yield a continuous curve of the classical type (dotted line, Figure 15) in which a reduction in temperature results in a continuous increase in yield stress as suggested by the data of Clough and Pavlovic[8] (Figure 2). In the present investigation two smooth curves were found which intersected at approximately -125°C, implying that there are two different temperature dependencies of the yield stress, applying over different ranges of low temperatures. That this is, in fact, the case is illustrated by replotting the yield stress (δ_y) versus temperature data in the following forms: (a) δ_y versus reciprocal absolute temperature (Figure 16), and (b) a log plot of δ_y versus reciprocal absolute temperature (Figure 17).

It is immediately obvious that a plot of δ_y versus $1/T$ does not yield a straight line, but rather two distinct intersecting curves. The points on the log plot of δ_y vs. $1/T$, on the other hand, can be fitted to two intersecting straight lines with relatively minor deviations from a linear correlation at all temperatures except those in the region of the intersection.

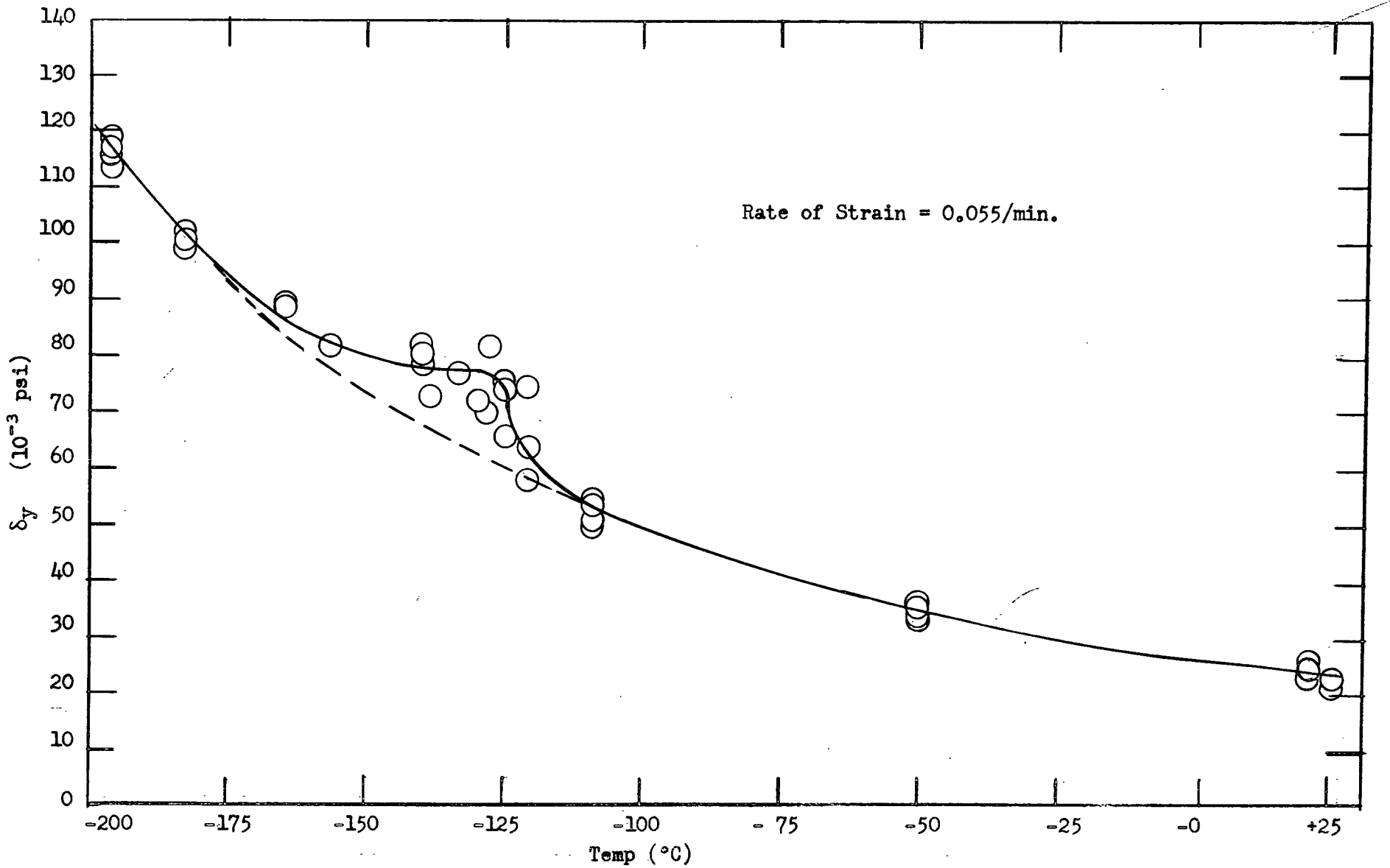

Figure 15. Yield Stress VS Temperature for Single Crystals

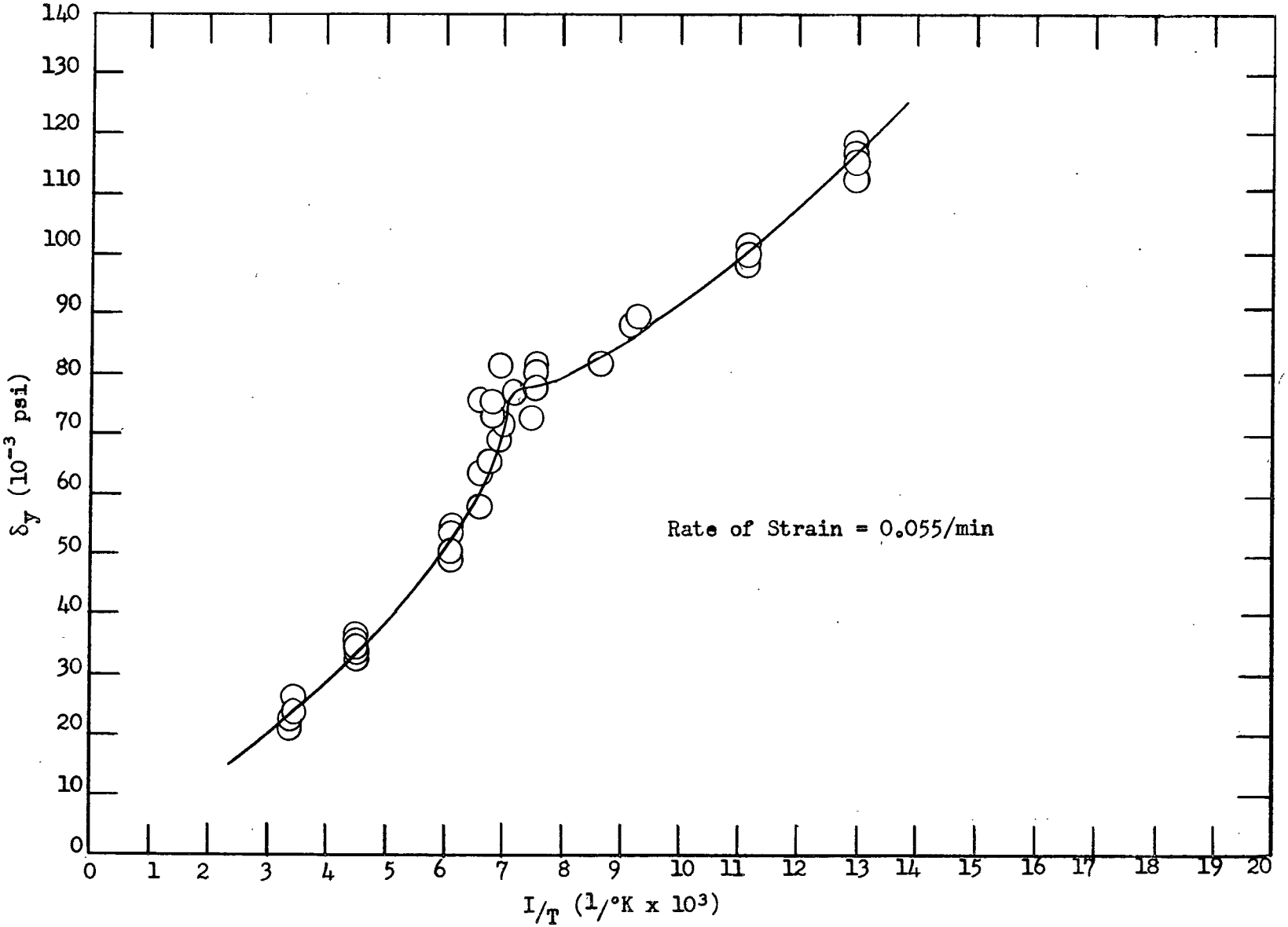

Figure 16. Yield Stress VS Reciprocal Temperature for Single Crystals

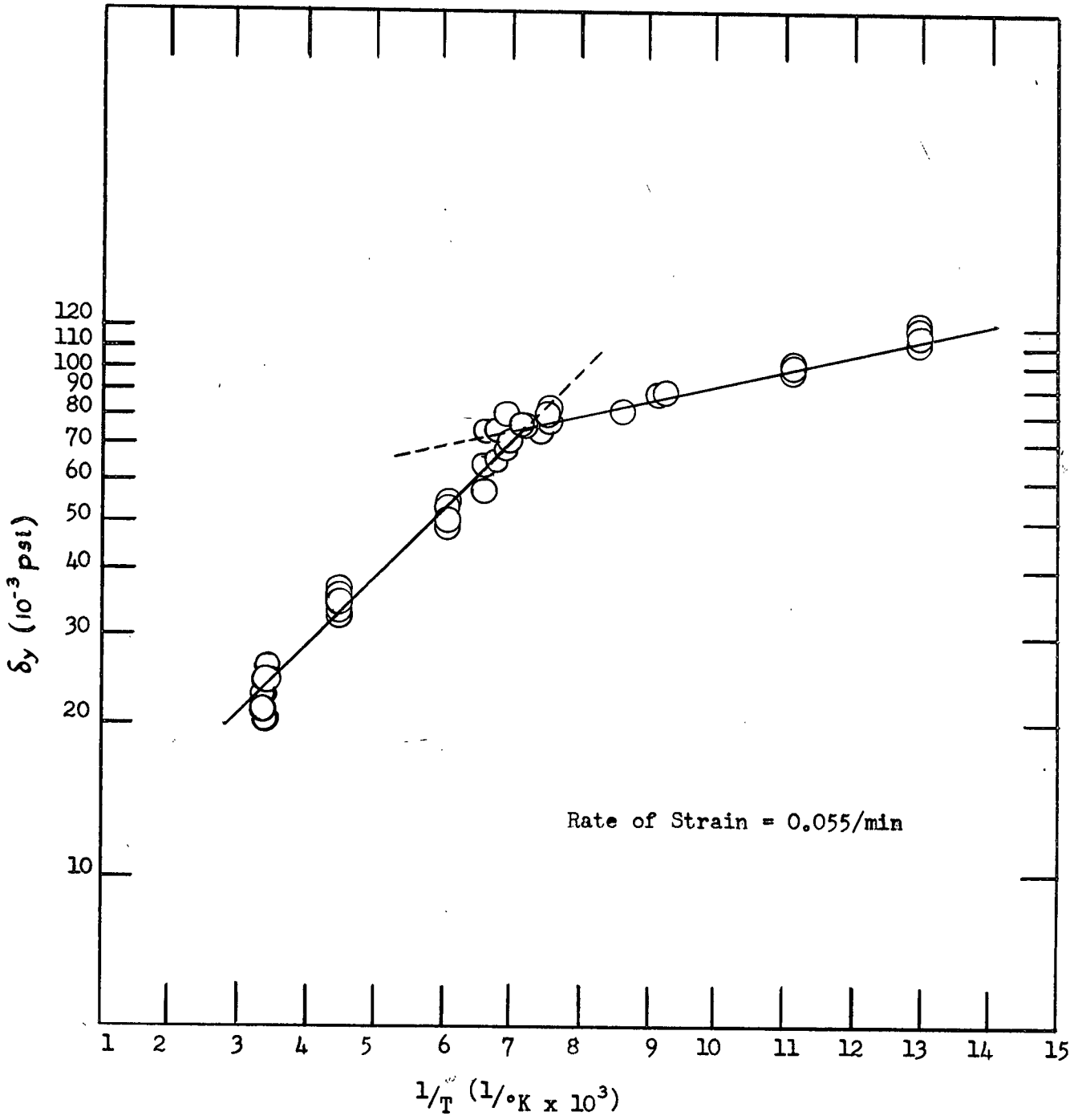

Figure 17. Log plot of δ_y VS Reciprocal Temp. for Single Crystals

There are currently two schools of thought concerning the temperature dependence of yield stress. Zener and Holloman[16] on the basis of tests predict a thermally-activated process obeying approximately an equation of the form

$$P = \dot{\varepsilon} e^{\frac{-Q}{RT}}$$

where

P = a reaction parameter

$\dot{\varepsilon}$ = strain rate

Q = 'activation energy' for flow

The equation which Zener[16] postulated will be presented in detail shortly.

Fisher[11] interpreted the Cottrell-Bilby theory of yielding[20] as indicating that yield stress should be a function of the form

$$\delta_y \left(T/_{G^2}\right) = \text{constant}$$

where G = shear modulus.

Zener's theory is based on the assumption that Q is relatively insensitive to changes in strain rate and temperature, whereas Fisher's theory is based on the assumption that G, the shear modulus is independent of temperature.

Zener and Holloman[16] illustrated that the tensile flow stress, δ_y, of steel could be expressed in terms of two variables only; ε, the strain, and the parameter P mentioned previously. Since, by Zener's theory,

$P = \dot{\varepsilon} e^{-Q/RT}$, it may be deduced that if Q is relatively insensitive to changes in $\dot{\varepsilon}$ and T over the range of temperature studied, then δ_y should be approximately equal to $e^{1/T}$, that is

$$\delta_y \sim e^{1/T}.$$

if strain (ε) and strain rate ($\dot{\varepsilon}$) are held constant. If log δ_y were then

plotted against reciprocal temperature, a straight line would result. Previously published results of tensile tests for steel,[16, 17] molybdenum,[18] and tungsten[19] all body-centered cubic metals, have indicated that the Zener hypothesis is correct in the temperature range over which yield strength is found to be particularly temperature sensitive.

Fisher[11] illustrated that the tensile flow stress, δ_y, of steel may be expressed in terms of the temperature and shear modulus only, in the manner described previously. According to Fisher's theory, a plot of δ_y against reciprocal temperature should yield a straight line. This postulate was supported by considerable low temperature tensile data obtained for iron and molybdenum by other investigators, and interpreted by Fisher[11].

The data fits Fisher's theory extremely well at temperatures above -140°C, but show marked deviations at temperatures below -140°C. This appeared to be true for both molybdenum and iron. The departure from Fisher's calculated curve closely resembles the curves found in the present investigation, as is evidenced by Figure 18.

Clough and Pavlovic[8] plotted their data in both ways, and found that Fisher's theory was obeyed, and that Zener's theory gave a systematic deviation from linearity. It should be remembered, however, that this work is subject to suspicion, since the methods of specimen preparation and mounting, as well as the type of tensile machine used apparently obscured the yield phenomena.

Loomis and Carlson[9] made no attempt to correlate their data in any way, but an attempt by the author to do so has indicated that any agreement with Fisher's theory is out of the question. A reasonable degree of agreement with the Zener hypothesis was found, but the limited number of experimental points involved made precise correlation difficult.

The results of the present investigation imply that the mechanism responsible for the temperature dependence of the yield point changes abruptly at a temperature between -125° and -132°C.

This suggests that in a narrow temperature range, a change takes place in the process or processes by which Frank-Read sources become unpinned from their surrounding impurity atmospheres, releasing dislocation loops which may then travel through the lattice. Three possible mechanisms whereby the curve of Figure 15 may be explained are given later in this thesis.

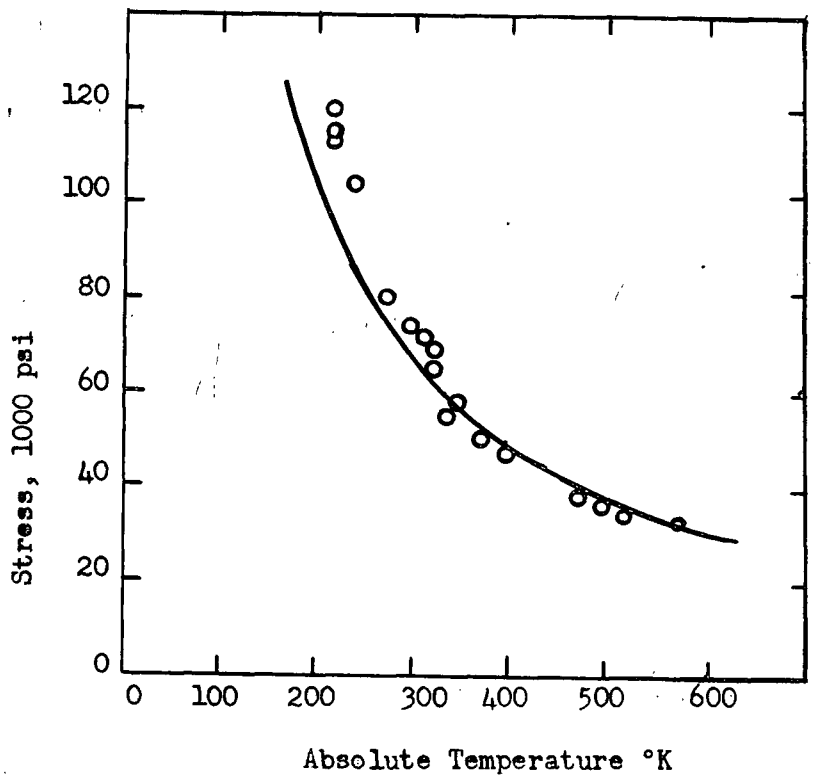

Figure 18. δ_y versus temperature for Annealed Molybdenum, after Fisher[11]

2. Flow Stress

The definition of flow stress is much more difficult than that of yield stress and for the purposes of this work it is defined as the point at which the sudden load-drop after yielding is stopped or slowed, and at which gross plastic flow begins. The load elongation curve of every crystal tested in this work displayed a relatively high yield point (see Figure 13). For high temperature specimens the flow stress was taken as the lowest point reached immediately following yielding. For low temperature specimens, this was not possible, since no minimum point was reached. In all cases, however, the curve underwent a change in slope after dropping sharply from the upper yield point. In these cases, the flow stress was taken at the intersection of lines drawn along the trace of the sharp drop after yielding and along the trace of the curve after the slope change. The results of these flow stress measurements are plotted in Figures 19, 20 and 21. It is evident from these graphs, that the phenomenon responsible for the pronounced discontinuity found in the curves for yield strength virtually disappeared or was obscured immediately after yielding occurred. The most noticeable change is that the log plot of flow stress against reciprocal temperature is no longer linear. It may, therefore, be concluded that the dual nature of the yield stress versus temperature relationship is concerned primarily with the high yield point phenomenon.

3. Elongation

Corresponding to the very sharp rise in yield strength in the temperature range between -105° and -125°C (Figure 15), is a sharp decrease in ductility (Figure 22). Figure 22 is a plot of percent elongation versus temperature. Considerable spread in the elongation values at any given temperature is exhibited. This is due to the fact that the specimens were

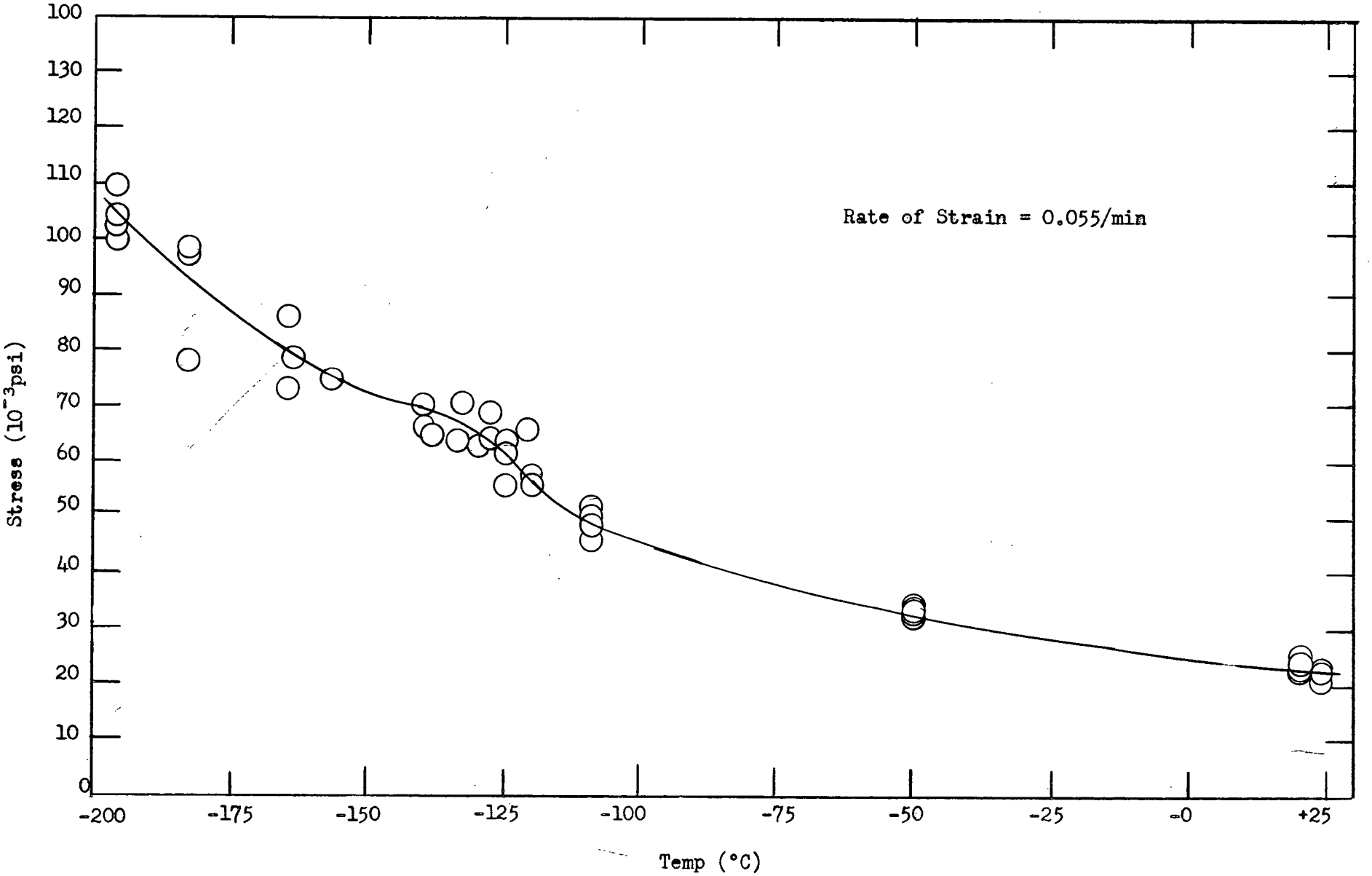

Figure 19. Flow Stress VS. Temperature for Single Crystals

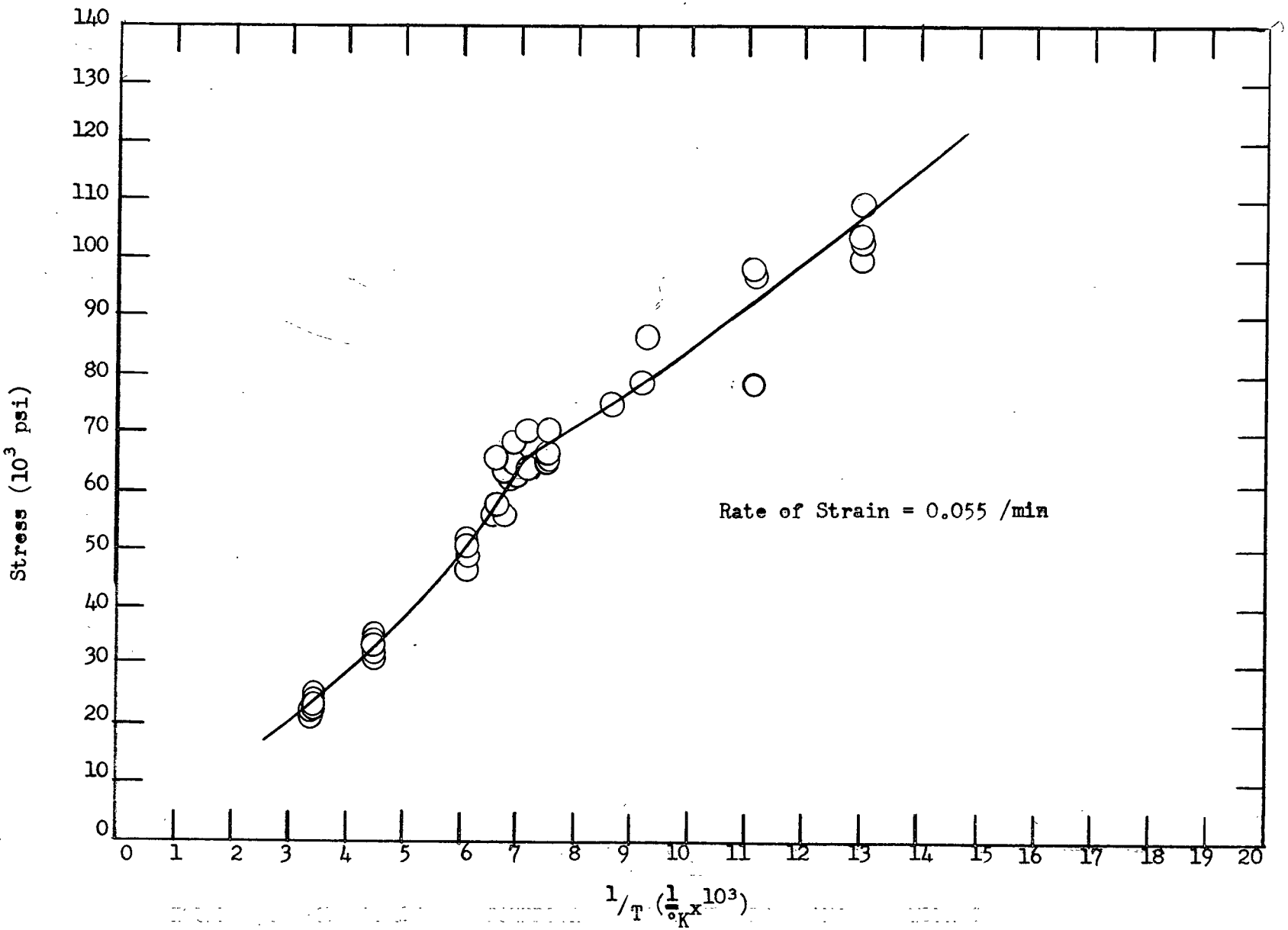

Figure 20. Flow Stress VS Reciprocal Temperature for Single Crystals

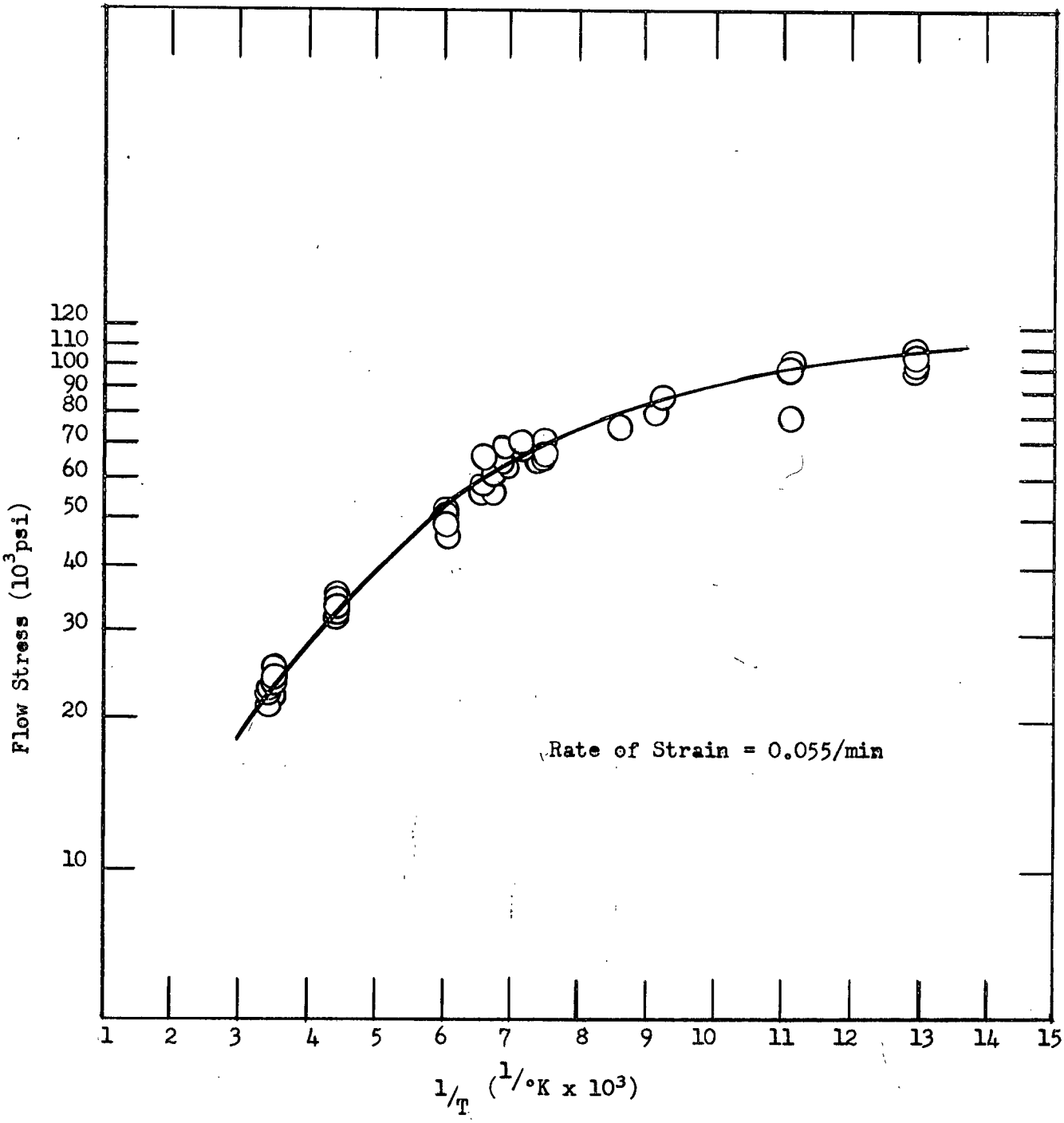

Figure 21. Log plot of flow stress VS Reciprocal Temperature for Single Crystals

single crystals, and much of the deformation occurred in the area immediately adjacent to the fracture. To clarify the relationship, an average value of percent elongation for each temperature was plotted, and superimposed on the individual specimen points.

B. SINGLE CRYSTALS - RATE OF STRAIN 0.0022/min.

Nine single crystals were tested at a rate of strain lower by a factor of $\frac{25}{250}$ than the previous rate in order to determine at least qualitatively the effect of strain rate on the yield point behaviour. The crystals were tested only at temperatures which were in the region of the intersection of the two lines in Figure 17. The results of these tests are shown in Figures 23 and 24. A discontinuity of the type observed at the higher strain rate is also plainly visible in this yield point data, although the small number of specimens used for this part of the work make it unreasonable to draw rigorous conclusions. The results indicate that the aforementioned mechanism change is not grossly affected by changes in rate of strain of the order involved in this work. The value of the yield strength at all temperatures was slightly lower at the lower strain rate, as it would be reasonable to expect.

C. POLYCRYSTALLINE SPECIMENS - RATE OF STRAIN 0.055/min.

Seven polycrystalline specimens were tested at a strain rate of 0.055 in/min. in order to determine qualitatively the effect of introducing grain boundaries and more random orientation. A high degree of preferred orientation existed in the specimens after deformation and annealing treatments. This would be expected, since the bars from which the polycrystalline specimens were machined were originally single crystals. Evidence of preferred orientation was the appearance of broken specimens, which in some cases showed a fracture similar to those found for single

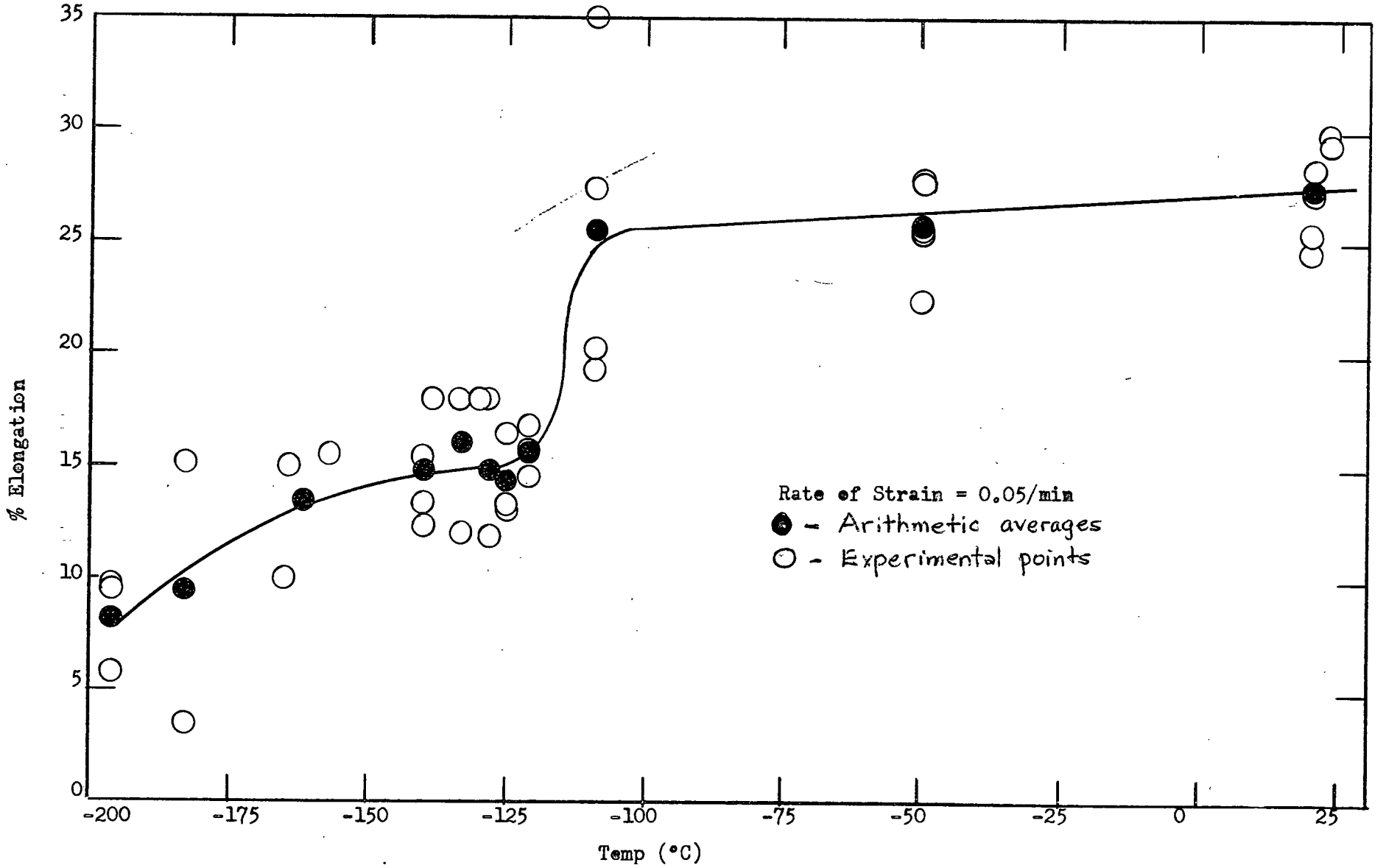

Figure 22. Percent Elongation VS Temperature for Single Crystals

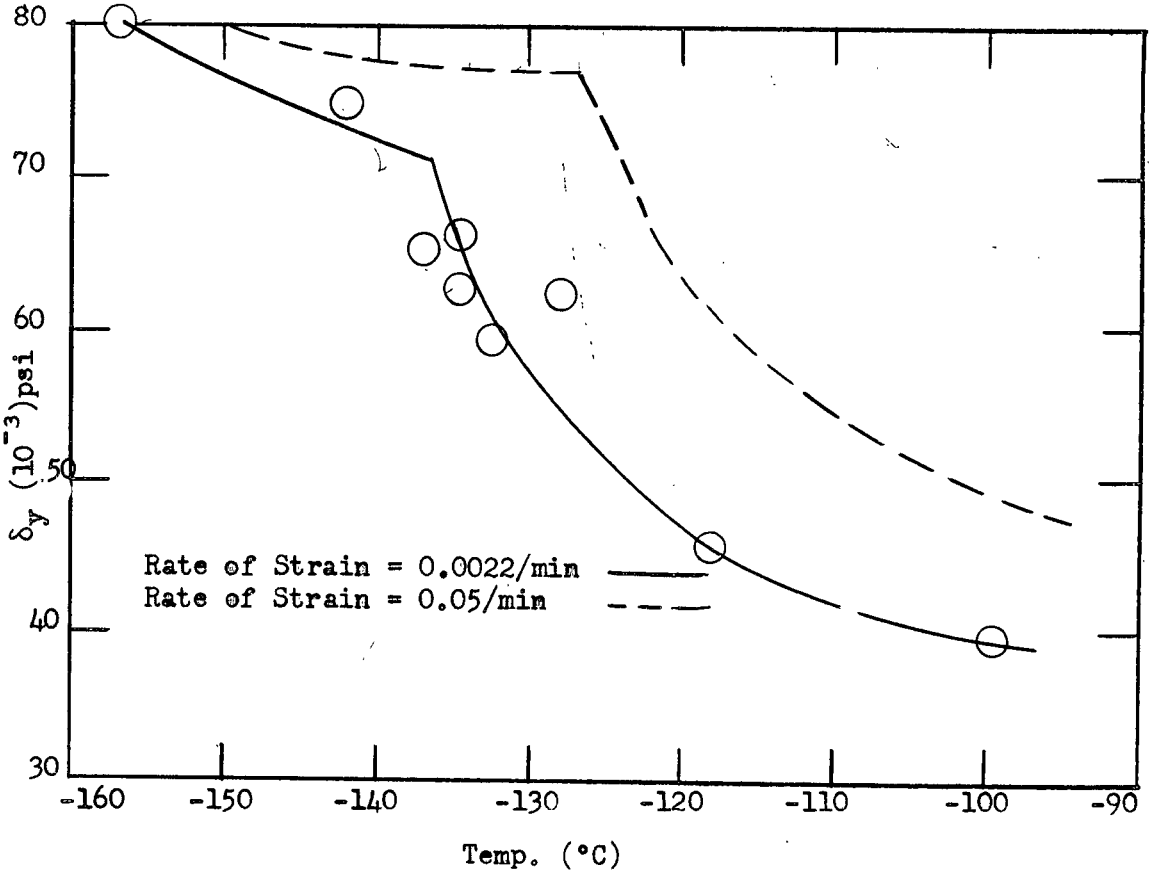

Figure 23. δ_y VS Temperature for Single Crystals

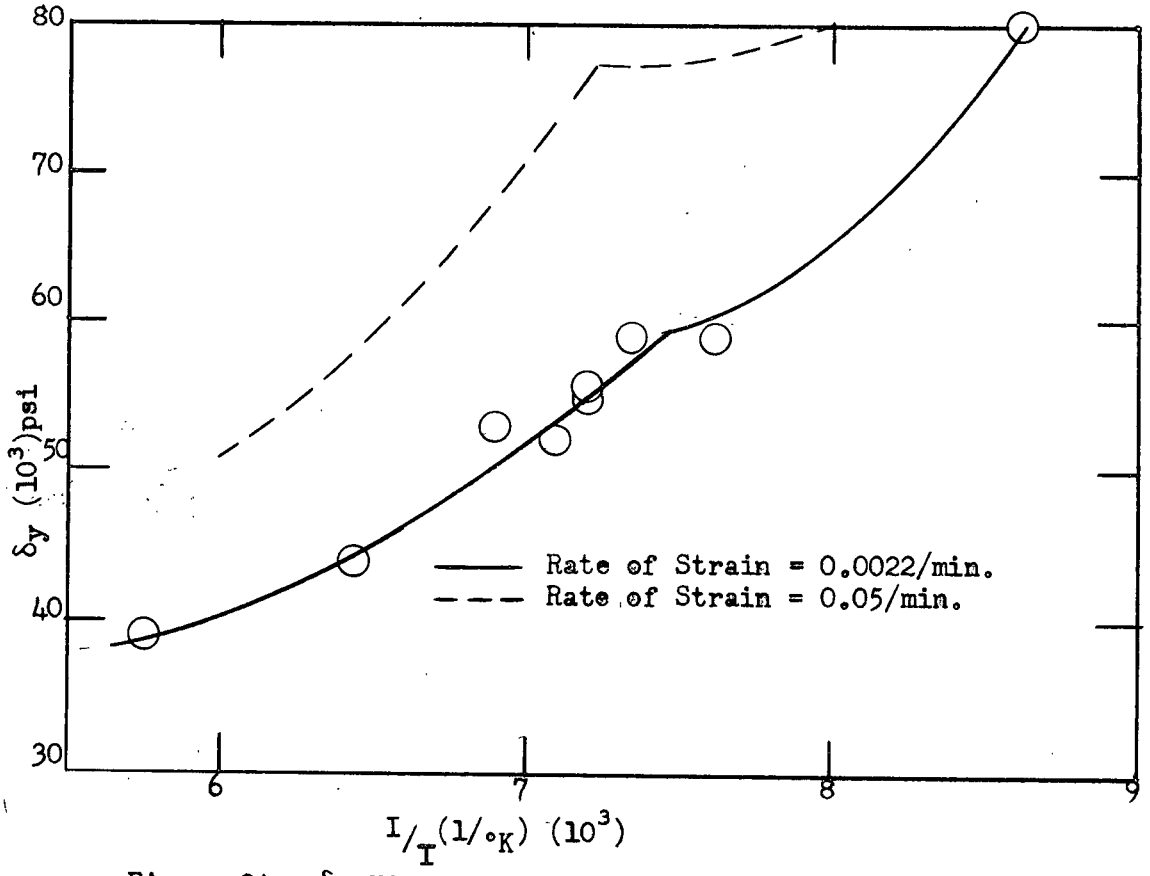

Figure 24. δ_y VS Reciprocal Temperature for Single Crystals

crystals (See Figure 14). Figures 25 and 26 show the results of plotting yield stress versus temperature and reciprocal temperature.

The limited amount of data indicates that the effect is greatly reduced in polycrystalline material. The slight effect evident may be due to the high degree of preferred orientation present in the polycrystalline specimens. If this is true, the yield stress versus temperature properties of vanadium are probably strongly orientation dependent. The data presented indicate that the yield stress of polycrystalline metal is much more temperature-sensitive at low temperatures (below the single crystal transition temperature) than is the yield stress of single crystals. Elongation data for polycrystalline specimens is not presented because of large scatter in proportion to the number of tests made.

D. ANALYSIS OF THE DEFORMATION MECHANISM

1. Slip System

The operative slip plane was found to be a plane in the ⟨110⟩ zone, always within a few degrees of {112}. This is different from the results of other investigators[21,22] working with single crystals of iron. Steijn and Brick[21] and Cox et.al.[22] made extensive studies of slip in single crystals of iron and found that slip always occurred in ⟨111⟩ directions on planes in the ⟨111⟩ zone, but not always on planes of low indices. This was referred to as 'banal' or non-crystallographic slip. A theory of slip in body-centered cubic metals, based on a hard sphere model, was proposed by Steijn and Brick[21]. In the model, slip on high index planes could be resolved into slip on planes of the forms {110} and {112}. Particular high-index planes would require a definite proportion of atom movements of each type.

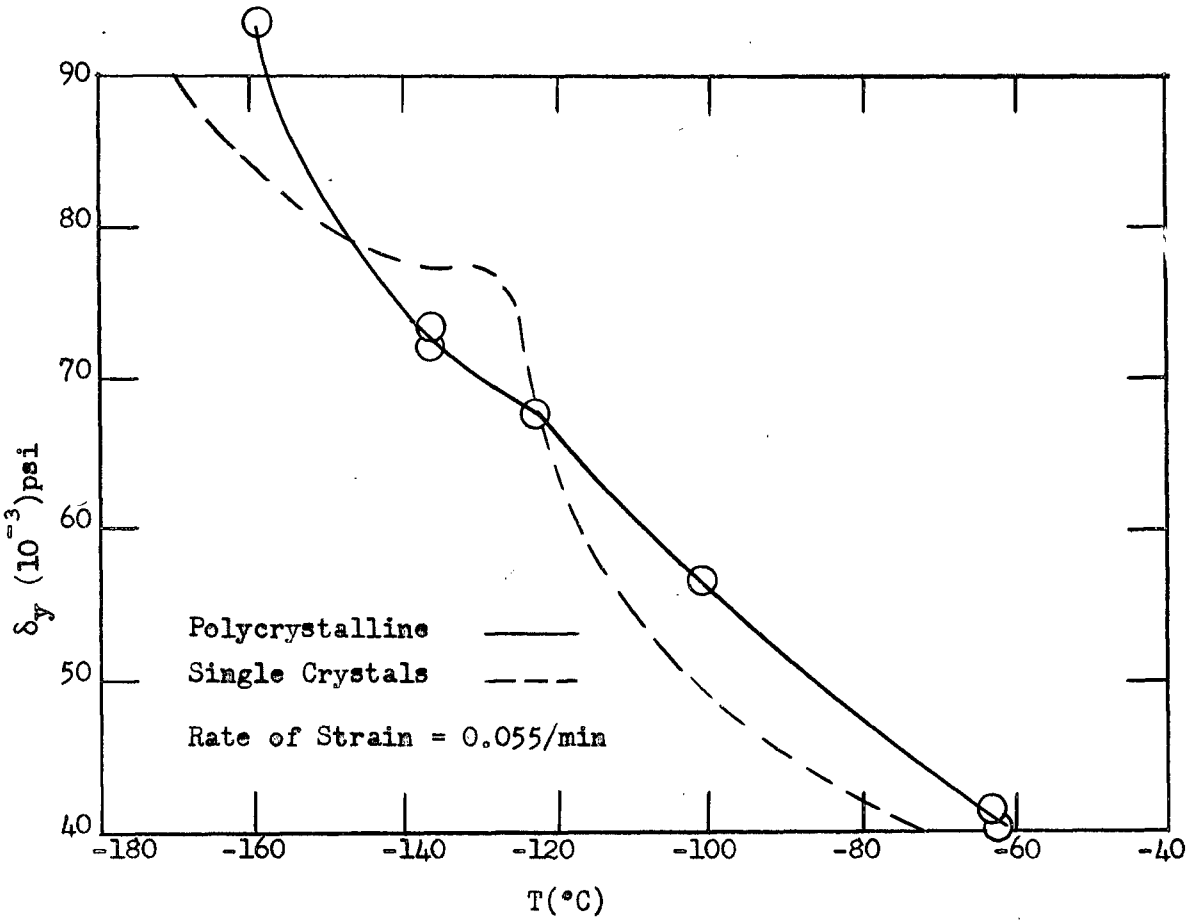

Figure 25. δ_y vs. Temperature for Polycrystalline Metal

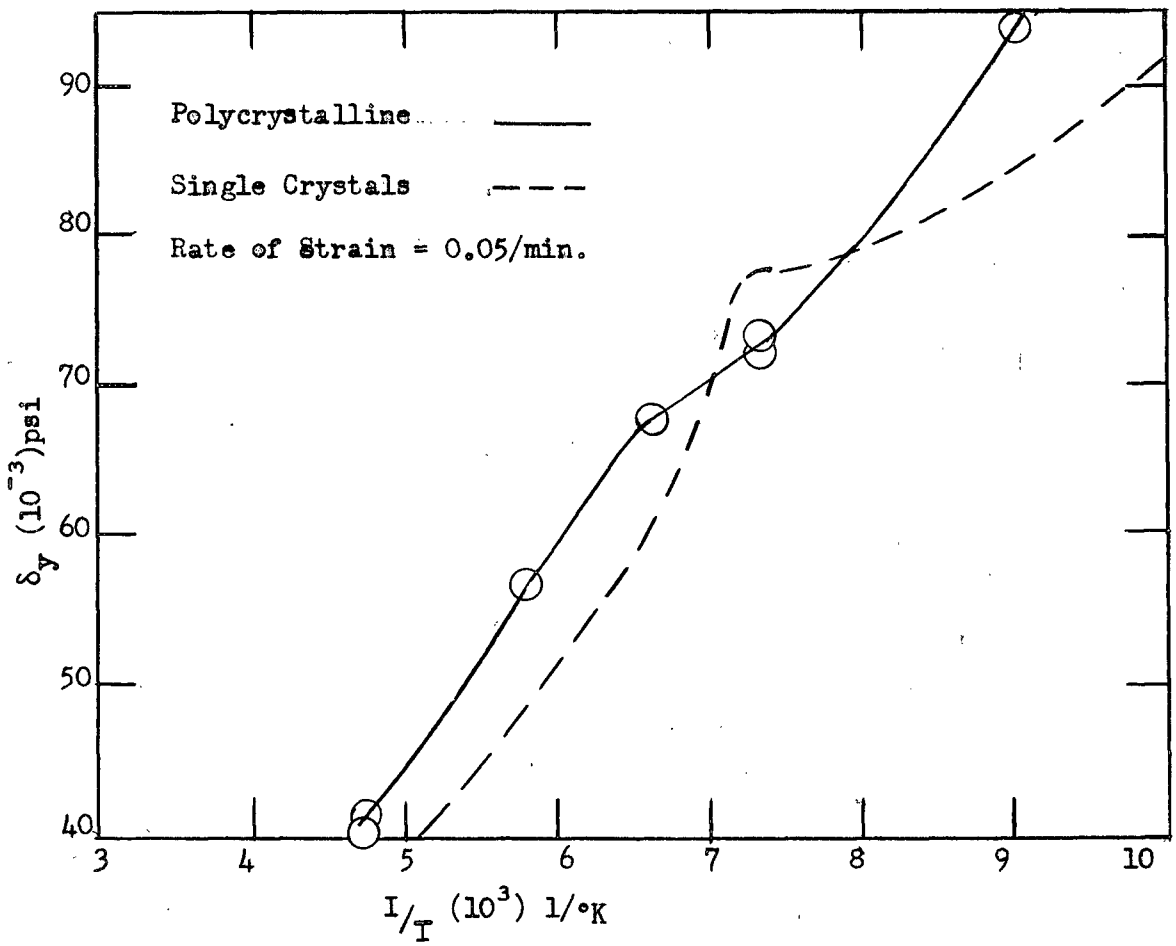

Figure 26. δ_y vs $I/_T$ for Polycrystalline Metal

It was thought initially that the dual nature of the yield stress curve was caused simply by a change in the deformation system at low temperatures. This was proved to be false on the basis of Laue back reflection photographs.

The complete orientations of the specimens were found from Laue photographs. The axial directions of the specimens were [110], and the orientation of all specimens was found to be that shown in Figure 27. The $[1\bar{1}0]$ direction appeared parallel to the knife edge of the broken specimen and the [001] direction appeared perpendicular to the knife edge. Hereinafter, Laue photographs which have been taken with the X-ray beam parallel to the $[1\bar{1}0]$ direction will be denoted as '$[1\bar{1}0]$ photographs' and photographs taken with the X-ray beam parallel to the [001] direction will be denoted as '[001] photographs'.

Specimens tested at temperatures both above and below the transition temperature were examined very carefully. X-ray photographs of a $[1\bar{1}0]$ type were taken of each specimen examined (Figures 28 and 30). Because of possible ambiguity concerning the similarity between $[1\bar{1}0]$ photographs and [001] photographs, advantage of the more obvious 3-fold symmetry of the [111] direction was taken. This was accomplished by photographing the specimen after it had been rotated through 35.3° from a position in which the $[1\bar{1}0]$ direction was parallel to the X-ray beam. The results of these photographs are shown in Figures 29 and 31. Angular measurements of slip traces indicated that the glide ellipse was at an angle of approximately 55° to 60° to $(\bar{1}10)$ planes (that is, the set of planes perpendicular to [110] and the specimen axis). These measurements were made from the slip traces shown in Figures 32 and 33. The low index planes {110} {112} and {123} are generally considered most likely to be operative slip planes for a body-centered cubic structure[24-26]. These planes are also the most likely

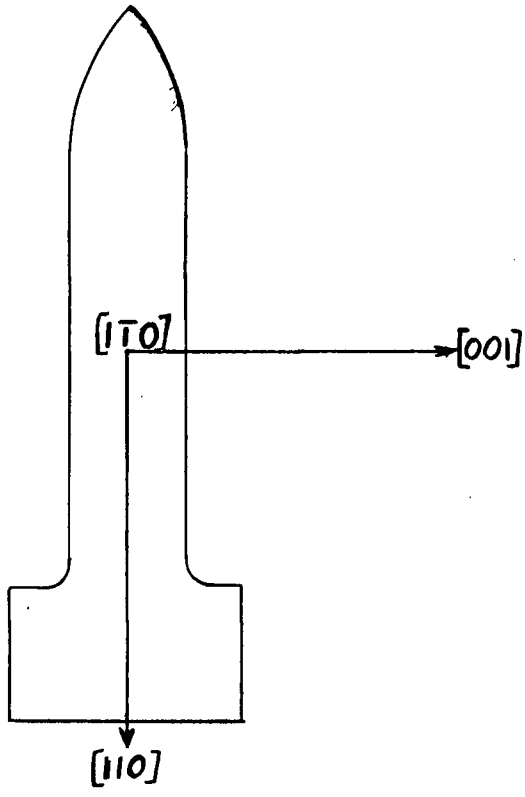

Figure 27. Orientation of Pulled Tensile Specimens

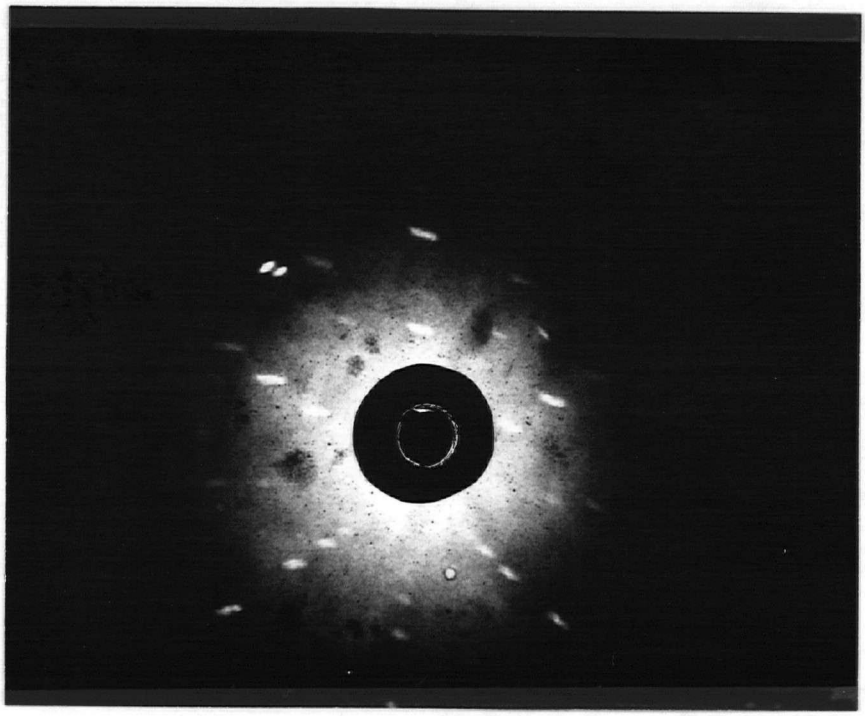

Figure 28. $[1\bar{1}0]$ Photograph of broken specimen tested at 24°C (V08T5)

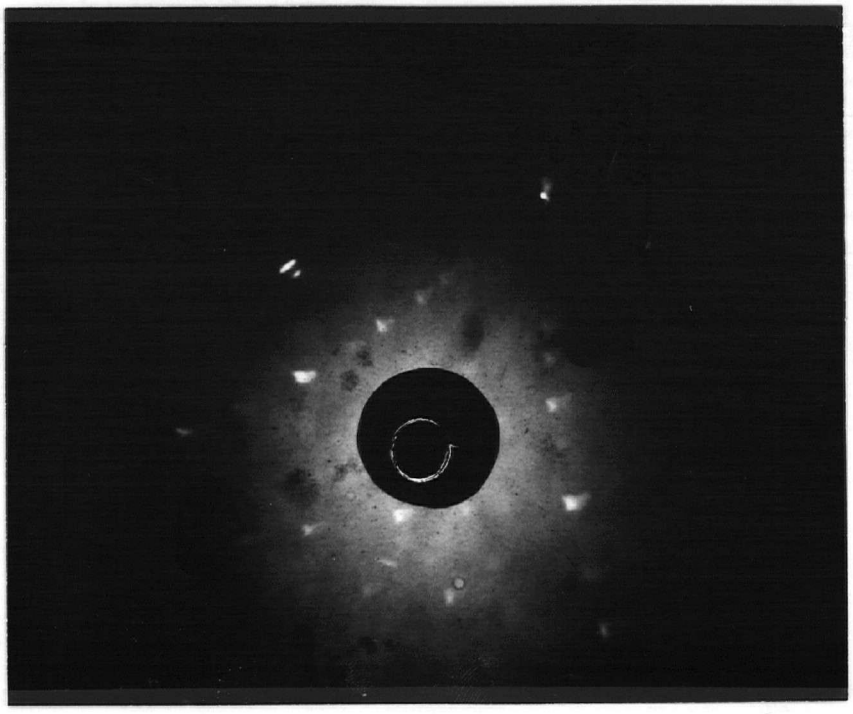

Figure 29. Specimen of Figure 28 rotated 35.3° towards [001]. Note the 3-fold symmetry of the [111] direction.

Figure 30. $[1\bar{1}0]$ Photograph of broken specimen tested at -183°C (V07T4)

Figure 31. Specimen of Figure 30 rotated 35.3° towards [001]. Note the 3-fold symmetry of the [111] direction.

slip planes in cases where non-crystallographic slips[21,22,27-29] is believed to occur.

In the present work it was found that slip occurred only on the $(\bar{1}\bar{1}2)$ and (112) planes. This was proven by the following crystallographic analysis, using the stereographic projection shown in Figure 34.

Examination of Figures 27 and 34, (the specimen orientation and the stereographic projection, respectively) showed that the (001) plane, the $(\bar{1}\bar{1}0)$ plane and the slip plane all lay in the same zone, namely the $[1\bar{1}0]$ zone. Therefore, planes of the $\{110\}$ form could not cause slip in this system. If $\{110\}$ planes were active slip planes, they would have to be $(0\bar{1}1)$ or $(\bar{1}01)$, operating in the $[111]$ direction. If these planes were operative, the knife edge of the deformed specimens would have to be oriented at 90° to the position in which it is actually found, both above and below the transition. The possibility of planes of the form $\{123\}$ serving as slip planes was also eliminated by a similar analysis. If $\{123\}$ planes were slip planes, the $(1\bar{1}0)$ reflection would not appear parallel to the knife edge, but rather offset by 10.9°. This was not found to be the case; the $(1\bar{1}0)$ reflection was always parallel to the knife edge.

In summary, the operative slip system was found to be $[111]$ $\{112\}$ over the whole range of temperature studied. Deformation was found to occur in the $[1\bar{1}0]$ zone, with (112) and $(\bar{1}\bar{1}2)$ planes as the only operative slip planes.

The measured angles of slip traces were slightly higher for the high temperature specimens (Figure 32) than for the low temperature specimens (Figure 33). This was probably due to the extensive elongation which the high temperature specimens underwent. The distortion of size and shape of the Laue spots of Figures 28 and 29 (high temperature specimens) was probably also a result of the extensive deformation of the high temperature specimens.

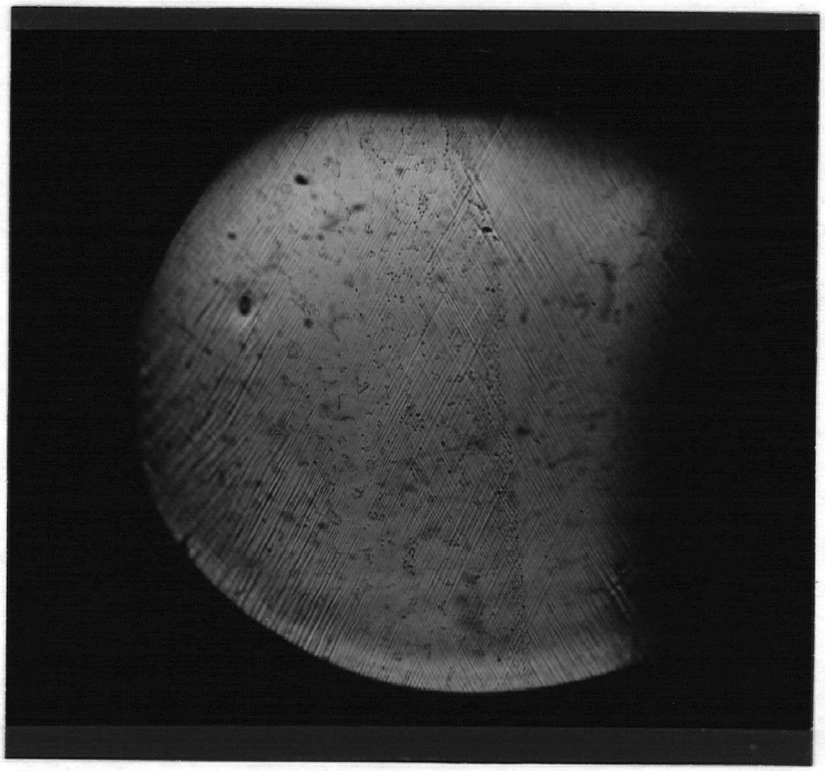

Figure 32A

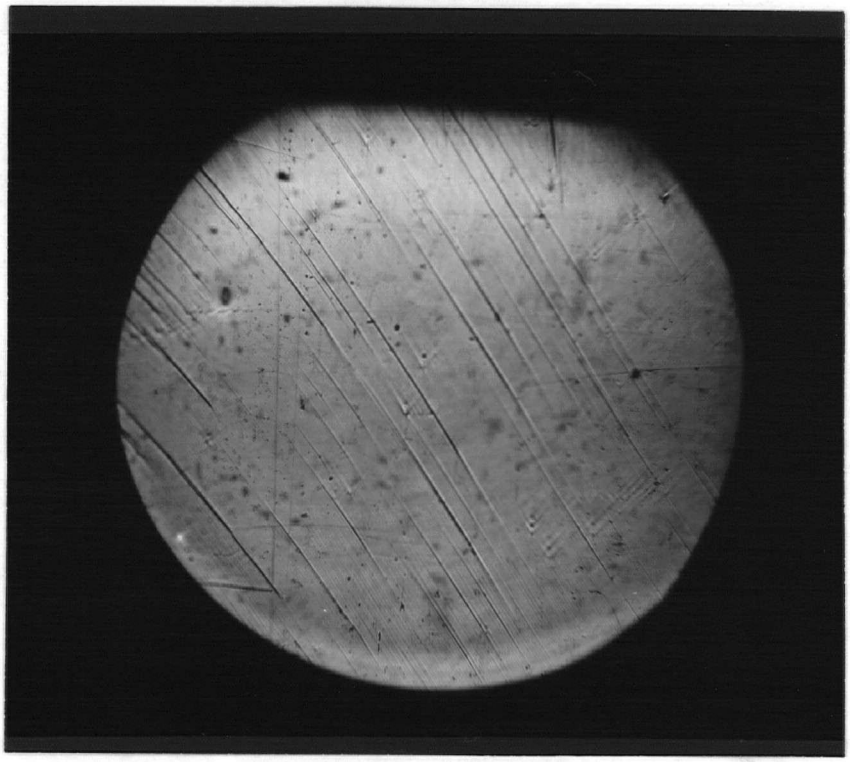

Figure 32B

Figure 32. Slip traces from specimens above the transition temperature.
Figure 32A is V08T3, tested at 24°C,
Figure 32B is V09T5, tested at -50°C.
Unetched, X125.

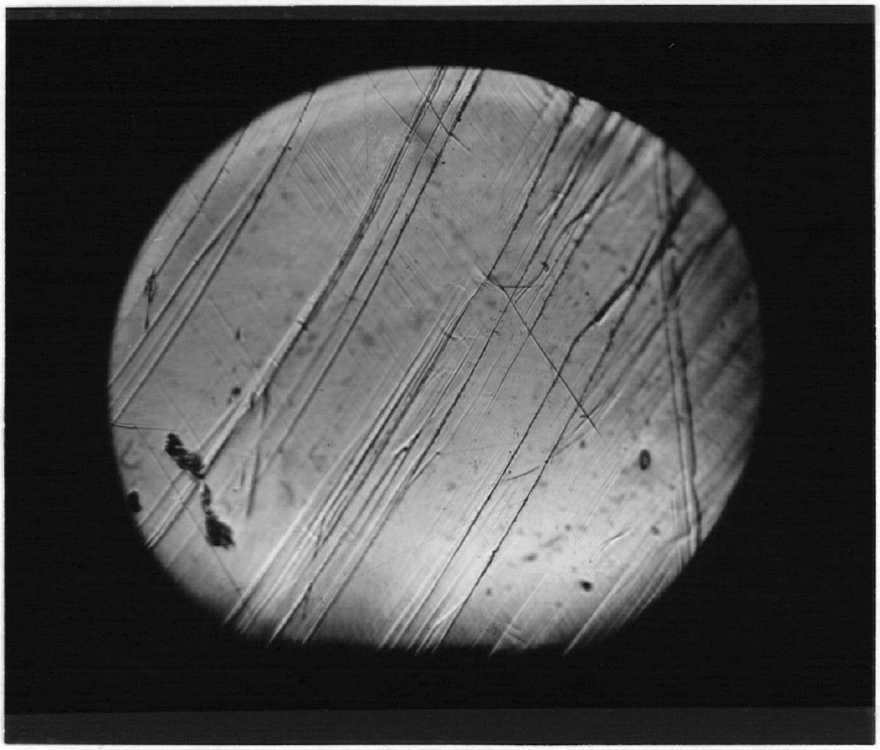

Figure 33A

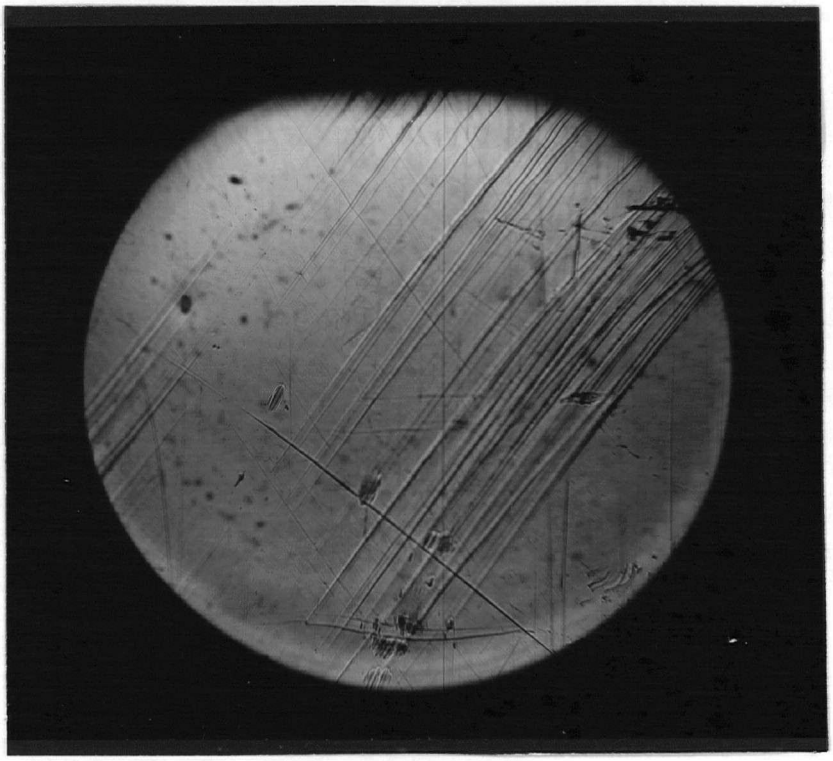

Figure 33B

Figure 33. Slip traces from specimens below the transition temperature.
Figure 33A is V07T4, tested at -183°C.
Figure 33B is V04T5, tested at -196°C,
Unetched X125

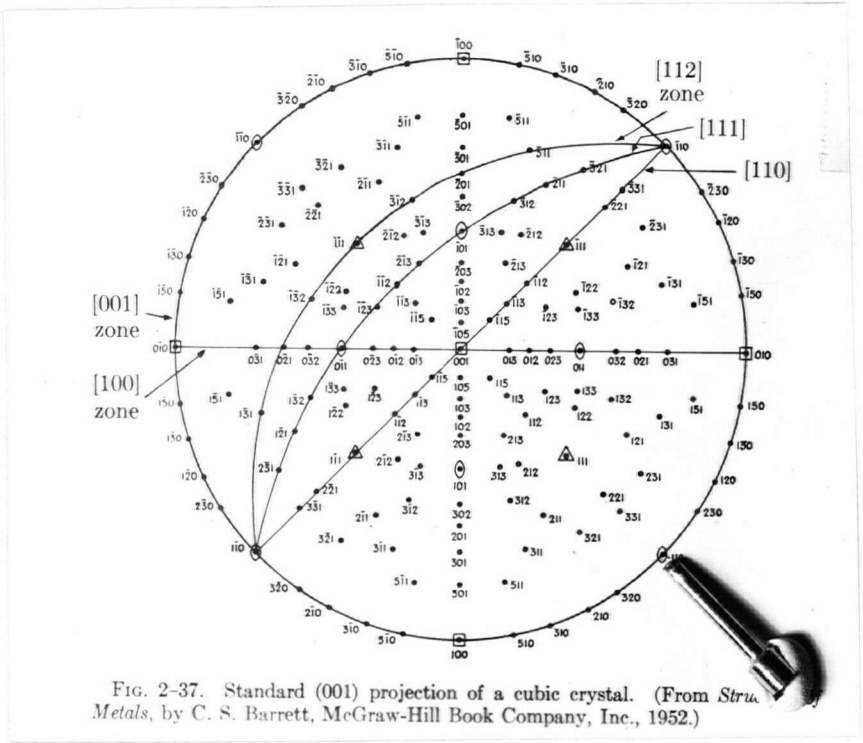

FIG. 2–37. Standard (001) projection of a cubic crystal. (From *Stru... Metals*, by C. S. Barrett, McGraw-Hill Book Company, Inc., 1952.)

Figure 34. Standard Stereographic Projection for the cubic system, showing the orientation of a standard tensile specimen with respect to the projection.

2. Twinning

Twins in vanadium have been observed by one investigator[8] and were reported as occurring on {112} planes which is the common twin plane for body-centered cubic metals. Exhaustive examination failed to reveal any markings on specimens in this work which could unambiguously be designated as twins. However, since the observed slip planes were found to be the same as the preferred twin planes, it is possible that slip and twin markings could occur coincidentally, and might therefore be indistinguishable.

It is possible that a change in deformation mechanism from slip to twinning could occur, and be responsible for the anomelous yield behaviour exhibited by vanadium single crystals. A recent paper by Adams, Roberts and Smallman[31] concerning the properties of niobium at very low temperatures reported the occurrence of large numbers of twins at very low temperatures or very high strain rates. However, niobium was found to twin 'reluctantly'.

Twinning in vanadium may be of a similar nature.

E. THE CRITICAL RESOLVED SHEAR STRESS

The resolution of simple tension in terms of the slip system is accomplished in the manner described below, with reference to Figure 35, which shows the fundamental quantities involved in the calculation.[26]

The slip direction for body-centered cubic metals is ⟨111⟩, and is affected by neither composition nor temperature. The active slip planes do depend on these quantities, and can be any of the planes of the form {110}, {112} or {123}, as long as the slip plane belongs to the zone of the slip direction. Let A be the area of the specimen, then $\frac{A}{\cos\phi}$ is the cross-sectional area of the slip plane. The force F is resolved in the [111]

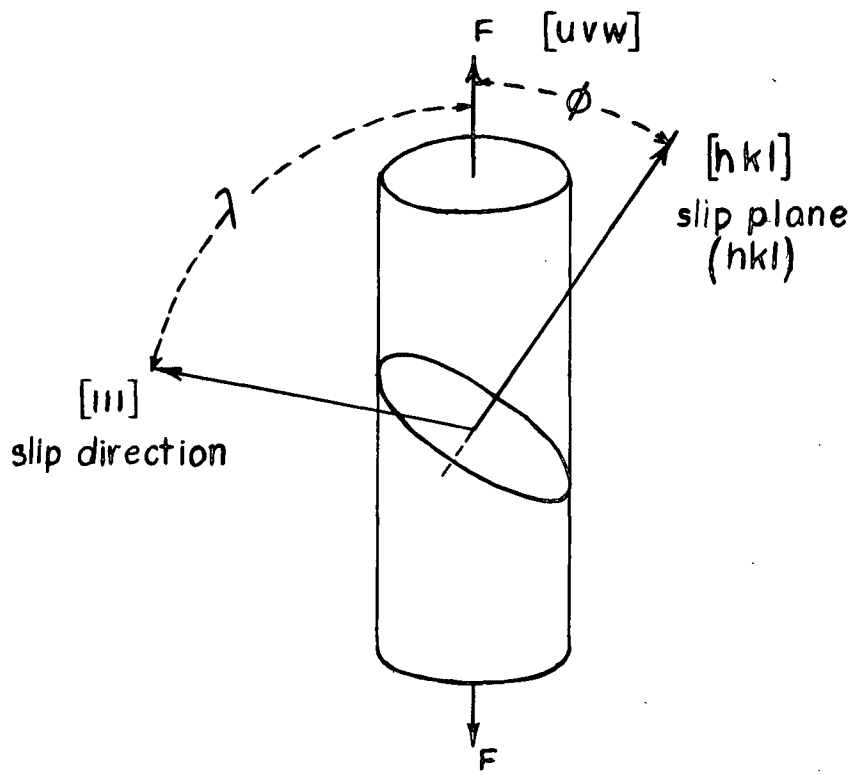

Figure 35. Fundamental quantities in the resolution of simple tension.[26]

direction and is equal to F cosλ , where λ is the angle between [111] and the tension axis.

Therefore: $$\delta_y^{[111]} = \frac{F}{A} \cos\phi \cos\lambda$$

By the analysis of the previous section, the slip planes are (112) and $(\bar{1}\bar{1}2)$, and from this, the angles ϕ and λ are 54°42' and 35° 18',

The values of the critical resolved shear stress are given in Appendix I and shown graphically in Figures 36, 37 and 38.

F. ELECTRICAL RESISTANCE

The possibility that a minor ordering or disordering reaction at the 'transition' temperature was the cause of the unusual temperature dependence of yield stress was examined by means of electrical resistance measurements taken between -196° and 0°C. All resistance measurements were made on a tensile specimen mounted in the testing machine, in such a way that stress could be applied. Measurements were taken on a Vernier potentiometer, and are accurate to $\pm$ 0.2%.

The results are recorded in Figures 39 and 40, and in Appendix III. Although a minor slope change was encountered at 100°K (-173°C), it is not believed that this is sufficient evidence for ordering. A similar change in slope of the resistivity curve was encountered by Rostoker[2] between -20° and -35°C, and Loomis and Carlson[9] (for bomb-reduced metal) between -70° and -80°C. The difference in the nature of the curve obtained in the present work is believed to be due to the higher purity of the metal used for these experiments.

The possibility of stress-induced ordering was examined by means of electrical resistance measurements taken at a given temperature and at different levels of stress. No appreciable change in resistivity between zero stress and the yield point was found.

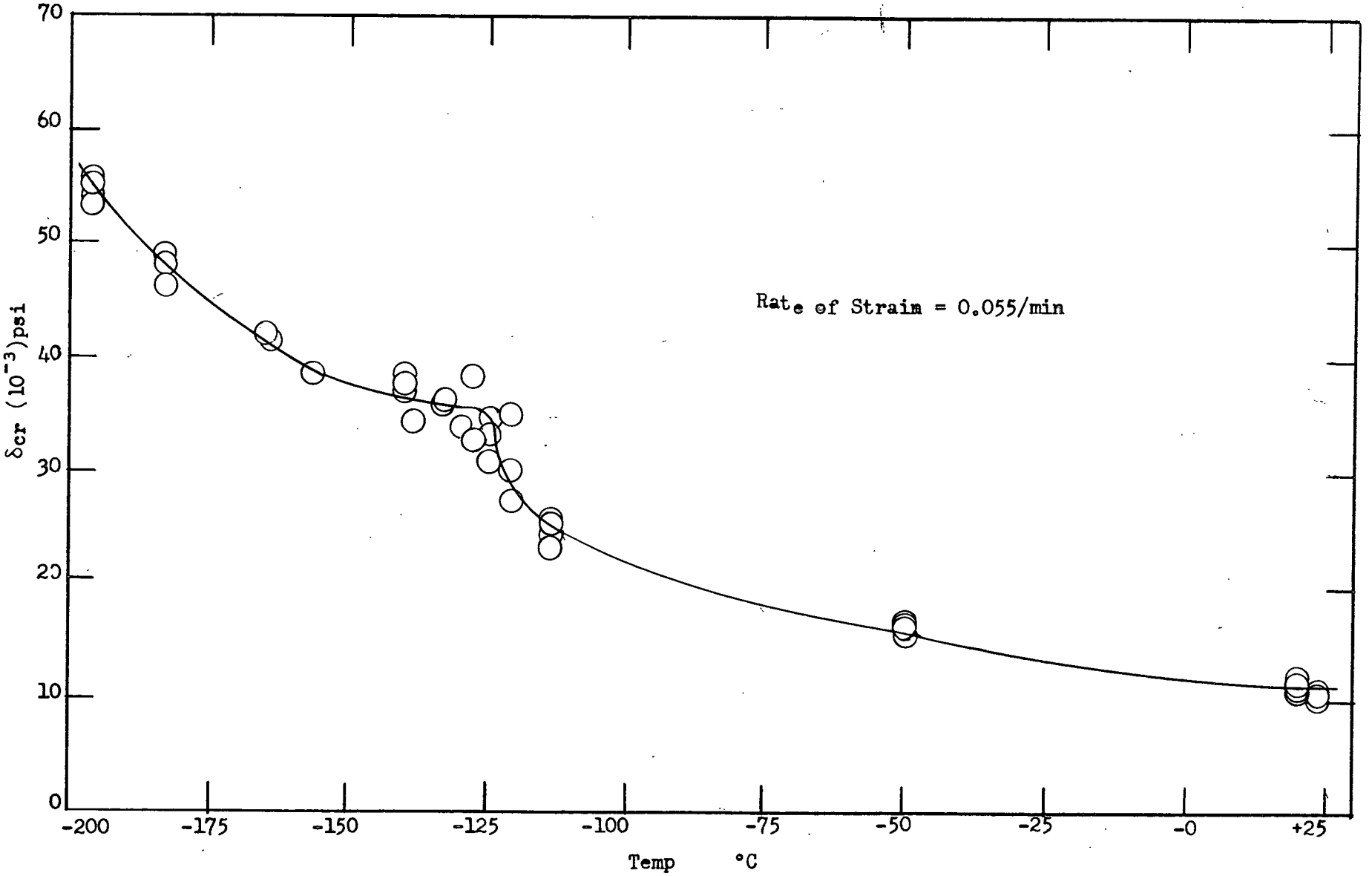

Figure 36. δcr VS Temperature for Single Crystals

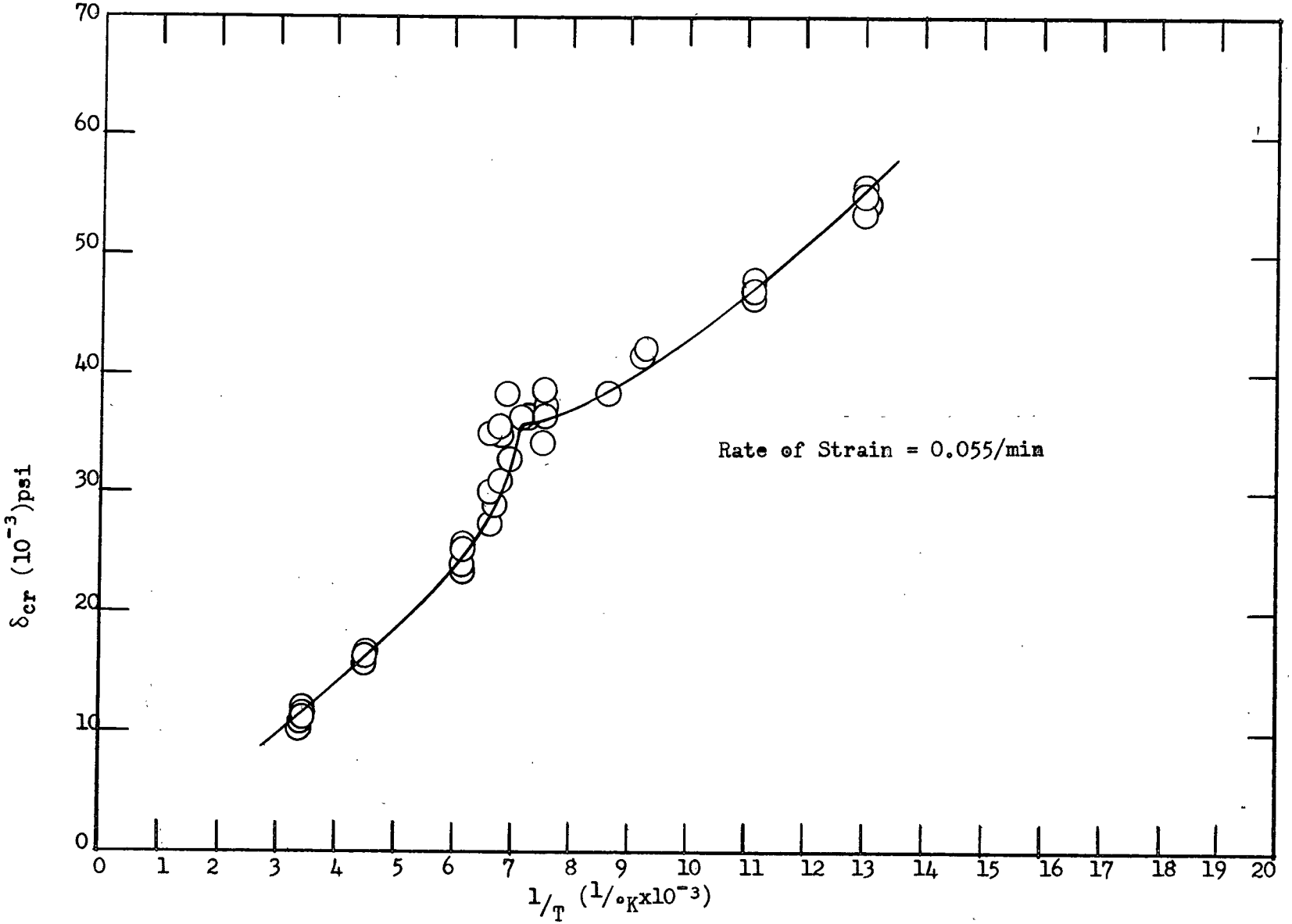

Figure 37. δ_{cr} VS Reciprocal Temperature for Single Crystals

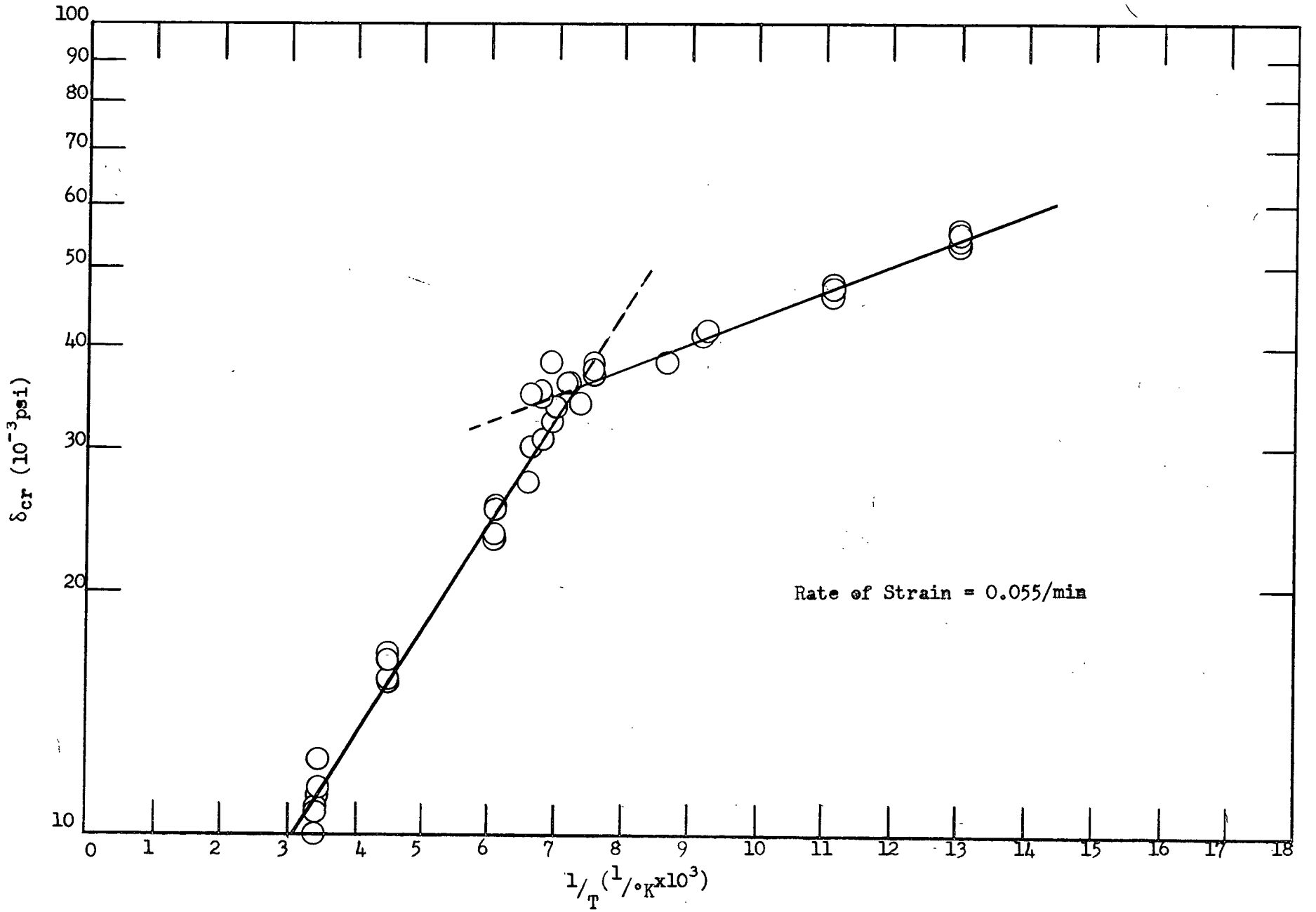

Figure 38 δ_{cr} VS Reciprocal Temperature for Single Crystals

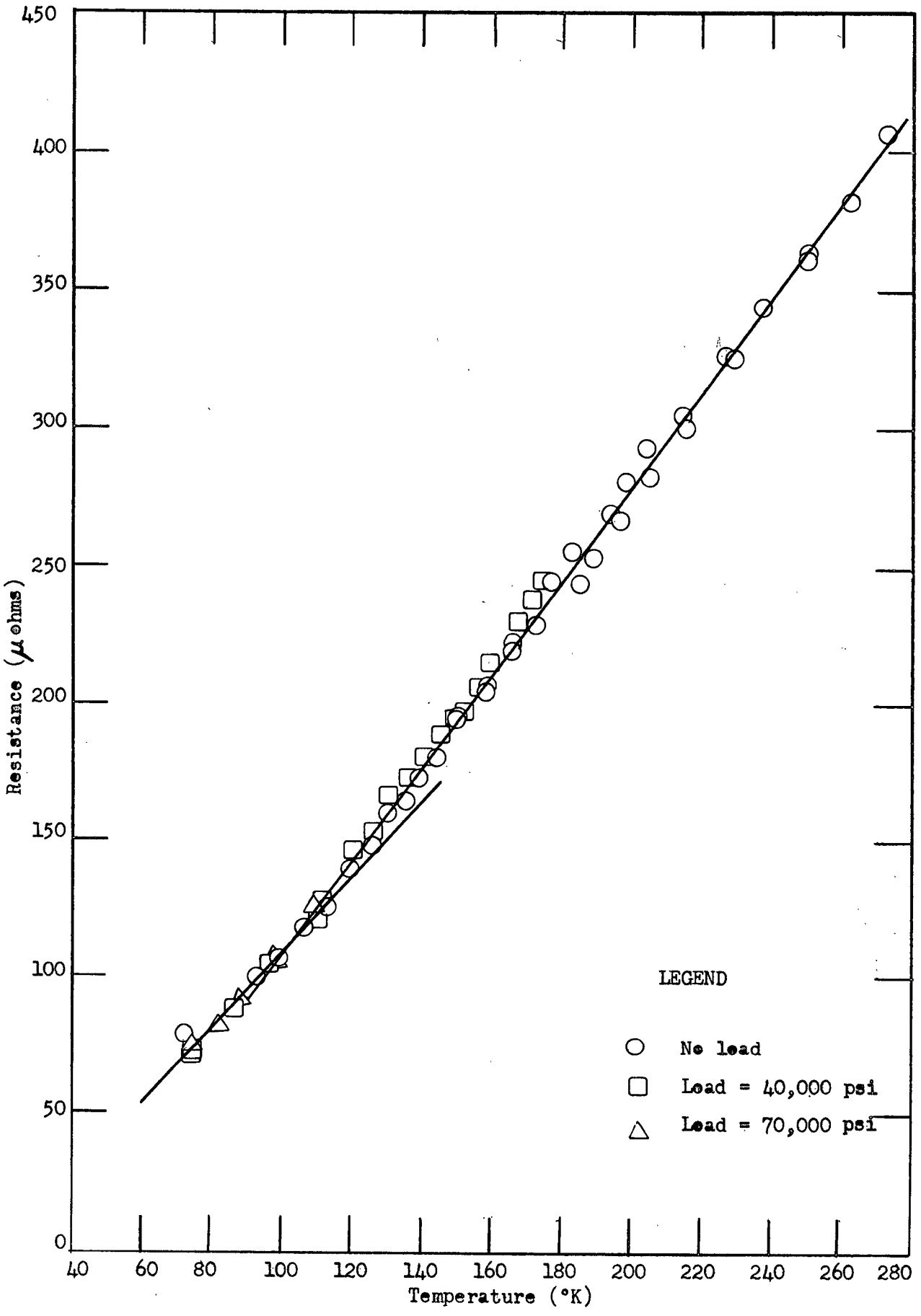

Figure 39. Electrical Resistance Versus Temperature for a Single Crystal

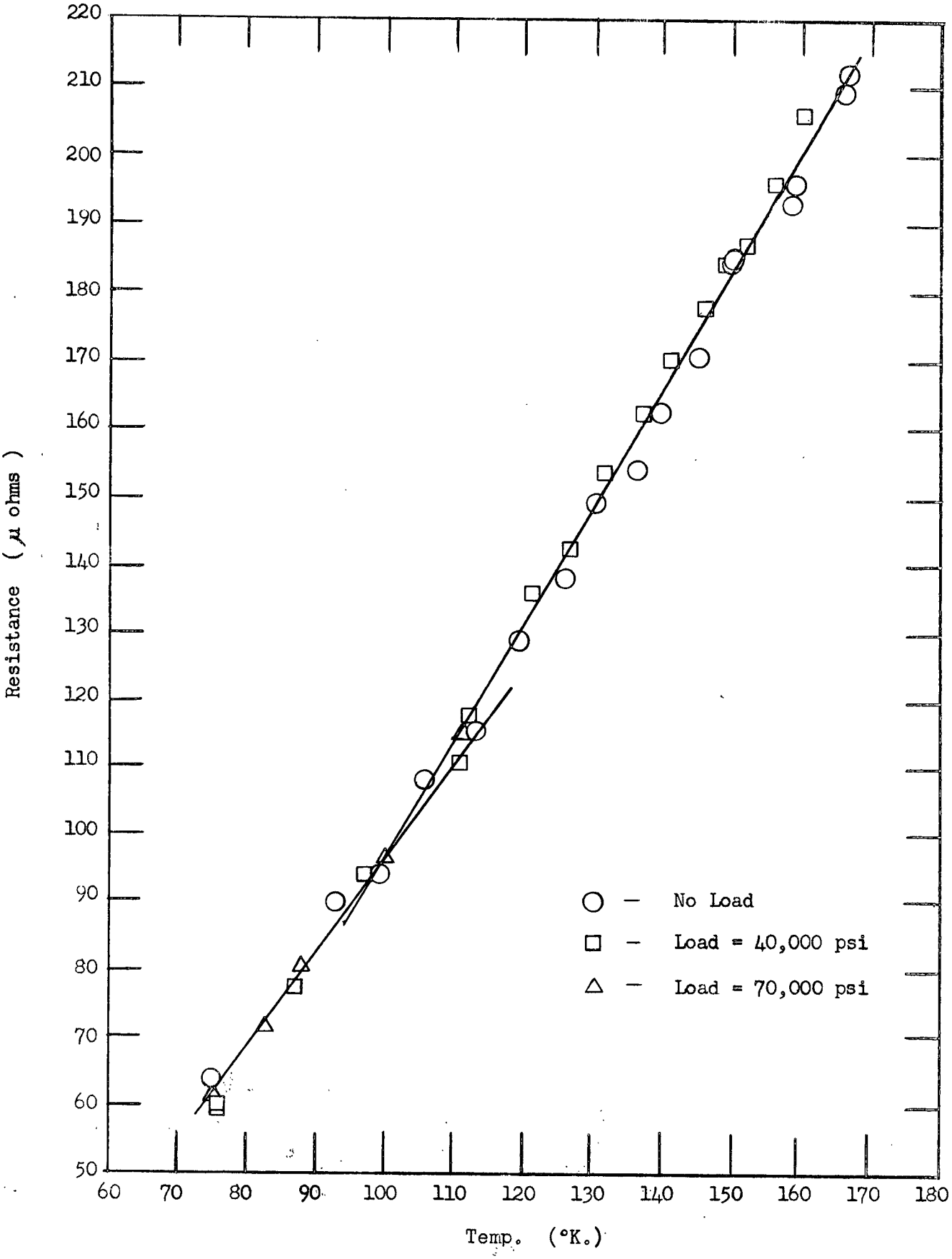

Figure 40. Enlargement of the Critical Region of Figure 39.

G. MICROHARDNESS

Microhardness measurements were made on every zone refined bar in an effort to establish some relationship between impurity content and microhardness. The purpose was to determine the uniformity of the zone refining process. Considerable hardness variation from bar to bar was encountered; however, hardness measurements were made on broken specimens polished after mounting in lucite, and a combination of the unavoidable misalligmment during mounting, and the variable plastic deformation present in the tested specimens is believed to be the cause of most of the differences. The hardness measurements made on specimens tested at high temperatures is not considered reliable for these reasons. It should be noted that hardness is an orientation-dependent property.

The value of the KHN for as-received vanadium was about 130-135, and for zone-refined metal about 105-110. Results of microhardness measurements are tabulated in Appendix IV.

The differences in hardness encountered did not appear to be reflected in the tensile results to any significant extent. A number of cases were encountered where specimens taken from a 'hard' bar were pulled at the same temperature as specimens taken from a 'soft' bar, but it was found that neither type of specimen had consistently higher or lower yield strength than the other type.

V. DISCUSSION

The present investigation has shown that high purity vanadium in the form of single crystals, conforms to the same general pattern of tensile behaviour as other body-centered cubic refractory metals in that it displays a very strong temperature dependence of yield strength, and a ductile-to-brittle (or semi-brittle) transition. It is now necessary to examine those factors which may explain the abnormal temperature dependence of yield strength exhibited by the single crystals, and which may account for the detailed differences between vanadium metal and the other body-centered cubic refractory metals.

A. REVIEW OF RESULTS

The anomalous temperature dependence of the upper yield stress of vanadium was found to be a thermally activated process, as evidenced by Figure 17 which shows the plot of log yield stress against reciprocal temperature. This behaviour is primarily a yielding phenomenon, since a plot of flow stress (Figures 19, 20, 21) against temperature did not show nearly as much departure from a smooth curve as did a plot of yield stress (Figures 15, 16, 17). Further, the flow stress data did not give a linear logarithmic plot.

Polycrystalline specimens tested under similar conditions showed a much less obvious anomaly (Figures 25, 26) and therefore the yield behaviour is believed to be dependent upon specimen orientation.

Single crystals tested at a lower strain-rate exhibited the abnormal behaviour very clearly (Figures 23, 24), although the discontinuity occurred at a lower stress and temperature. The yield stress, therefore, is also strain-rate dependent; an increase in strain rate resulting in an increase in 'transition' temperature.

X-ray data indicate that the slip system does not change over the range of temperature studied, so therefore the change in the temperature dependence of yield stress is not associated with a simple change of slip system.

Loomis and Carlson[9] studied a single crystal of crystal-bar vanadium at low temperatures by means of a Weissenberg camera in order to determine whether or not any form of allotropic transformation occurred. They reported that no change occurred to -115°C (the ductile-to-brittle transition occurred at -110°C). X-ray diffraction data presented by Loomis and Carlson indicated that vanadium exists in the body-centered cubic form down to -180°C. On the basis of this data, it may be assumed that no crystallographic change takes place in the range of temperature studied which could account for the abnormal temperature dependence of the yield stress.

B. POSSIBLE MECHANISMS

The above discussion restricts the possible mechanisms by which a discontinuity in the temperature dependence of yield stress can be explained. Three alternative mechanisms are suggested: (1) a change in deformation mechanism; for example, from slip to twinning, (2) a minor ordering or disordering reaction, or (3) a change in the manner in which dislocation becomes unlocked at the yield stress. Each of these possibilities will be discussed more critically in the following text.

1. Change in Deformation Mechanism

The shape of the plot of log yield stress against reciprocal temperature suggests the presence of two different thermally activated processes; with the higher temperature process having a higher activation energy. At the transition temperature the process having the higher activation energy (presumed to be slip) is replaced by a process with the

lower activation energy (presumed to be twinning). Adams, Roberts and Smallman[31] found evidence of gross twinning in polycrystalline niobium at very low temperatures; Cox, Horne and Mehl[22] and Steijn and Brick[21] found evidence of large amounts of twinning in iron single crystals at -196°C. In all cases reported, the twinning was accompanied by audible clicks in the specimen, and 'jerks' in the linear portion of the load-elongation curve. In the present investigation the same observations were made at -196°C and -183°C, but no evidence of twinning could be found on metallographic examination of the broken specimens. However since the slip plane identified in vanadium single crystals, and the twin plane (112) reported by Clough and Pavlovic[8] are coincident, it is possible that a combination of slip traces and twins were present, even though repolishing and etching failed to provide adequate evidence that this was so. Adams, Roberts and Smallman[31] reported that most of the twinning in niobium occurred during the very early stages of plastic deformation. In the present investigation, no low temperature tests were interrupted for the purpose of specimen examination, because of the difficulty in removing an unbroken specimen from the machine without spoiling the electropolished surface. Since considerable plastic deformation occurred before fracture, even at -196°C, it is possible that visible evidence of twinning was obscured by slip lines. Adams et.al. also reported a standard pattern of behaviour of all specimens pulled at 20°K; (a) that small amounts of slip interspersed between extensive bursts of twinning occurred in the early stages of deformation, (b) that a preponderance of slip with only occasional twinning occurred as deformation was continued, and (c) that the crystals displayed an ability to work-harden while deforming by slip. By this standard, any twinning which may have taken place in low temperature specimens may well have been obscured by subsequent slip deformation.

A theory of twinning in iron crystals by Biggs and Pratt,[32] developed from the Cottrell-Bilby theory[20] claims that twin nucleation is more difficult than twin propagation. The suggestion was made that twin nucleation is caused by a stress concentration which is brought about by the release of a burst of slip as a Frank-Read source breaks away from its atmosphere, causing the rapid piling-up of dislocations. Twins, once formed, may themselves act as barriers, allowing further piling-up of dislocations and further twin nucleation. When most of the Frank-Read sources have been released from their atmospheres, slip will no longer occur in bursts, and twin nucleation will no longer be possible.

A mechanism of this type could well account for the heavy appearance of the slip lines at low temperatures, Figure 33, and for the discontinuous temperature dependence of the yield stress.

The qualification must be made, however, that twins in niobium were not found until the temperature was reduced below -196°C, and not in abundance until 20°K was reached. Further it must be remembered that in the present investigation no concrete evidence that gross twinning had taken place was found, even though jerks in the load-elongation curves, and corresponding audible clicking noises occurred in many of the specimens tested at temperatures lower than -165°C.

2. Ordering Process

The occurrence of a minor slope change in the plot of electrical resistance versus temperature could possibly be due to an ordering or disordering reaction, although it is not considered likely because of the extremely small number of impurity atoms available to participate in the reaction. The ordering process is thought to be the occupation of preferred interstitial sites by atoms say, for example, of carbon. It is suggested that this situation may be brought about by contraction of the

lattice due to applied stress and thermal contraction, such that at the transition temperature, the occupied sites become too small to accommodate the impurity atoms, which are then forced to take up new ordered positions in the lattice. That this type of reaction occurred would be most difficult to prove, particularly since it is unlikely that resistivity measurements would detect an ordering reaction of such small magnitude.

A mechanism of this type could, however, explain partially the log plot of yield stress versus reciprocal temperature. The change could be considered analogous to an alletropic transformation, in that it would be virtually diffusionless (a necessary condition because of the improbability of diffusion taking place at the low temperatures involved). It would merely involve the transfer of interstitial atoms from one site to an adjacent or nearly adjacent one of more suitable dimensions. Since the change in slope of the resistivity curve was found to occur below the transition (-170°C), thus allowing the transformation to take place before the change is noticeable, this mechanism is not impossible. For the reasons stated earlier, however, it would appear unlikely.

3. Dislocation Breakaway

The Cottrell-Bilby theory of yielding in iron[20] postulates the migration of impurity atoms to Frank-Read sources where they form atmospheres. When an applied stress exceeds the pinning force, the dislocation loops break away from the atmospheres, thereby causing the heterogeneous yielding characteristics found in body-centered cubic metals.

A mechanism which could explain the temperature dependence of yield stress of vanadium single crystals found in this investigation requires that two interstitial impurity species form atmospheres around dislocation sources.

It is assumed that each impurity species has an independent locking effect on dislocations which it surrounds. Thus it can be considered that the effect of one impurity on the temperatures dependence of yielding in vanadium is different from that of any other impurity. Figure 41 is a hypothetical plot of the yield stress-temperature relationship due to each of two arbitrary interstitial species assuming the Zener hypothesis[16] applies. It is probable that the vertical position of each of the two lines will be dependent on the relative concentrations of the two species. The slope of any line will be characteristic of the impurity, and determined by factors such as atomic diameter and possibly valency.

According to Figure 41, the stress necessary to overcome the locking effect of one species (impurity A) is less at high temperatures (above T_1) than the stress necessary to unlock dislocations from impurity B. At temperatures less than T_1, the reverse is true, and the minimum stress required to initiate yielding is determined by the locking effect of impurity B. This implies that a temperature may exist for certain relative concentrations of the two impurities at which the locking effect of one impurity becomes less significant than that of the other impurity, leading to a discontinuity in a plot of yield stress versus temperature.

A number of observations in the present work give strong support to this suggested mechanism.

Among these experimental data which this hypothesis explains satisfactorily are the following:

1. The anomaly found in the temperature dependence of yield stress in the present work.

2. The scatter of the results observed in the vicinity of the intersection of the two straight lines in Figure 17. This scatter would be expected in a region where the stress to free dislocations pinned by either of two impurities is of the same magnitude. Hence, very minor

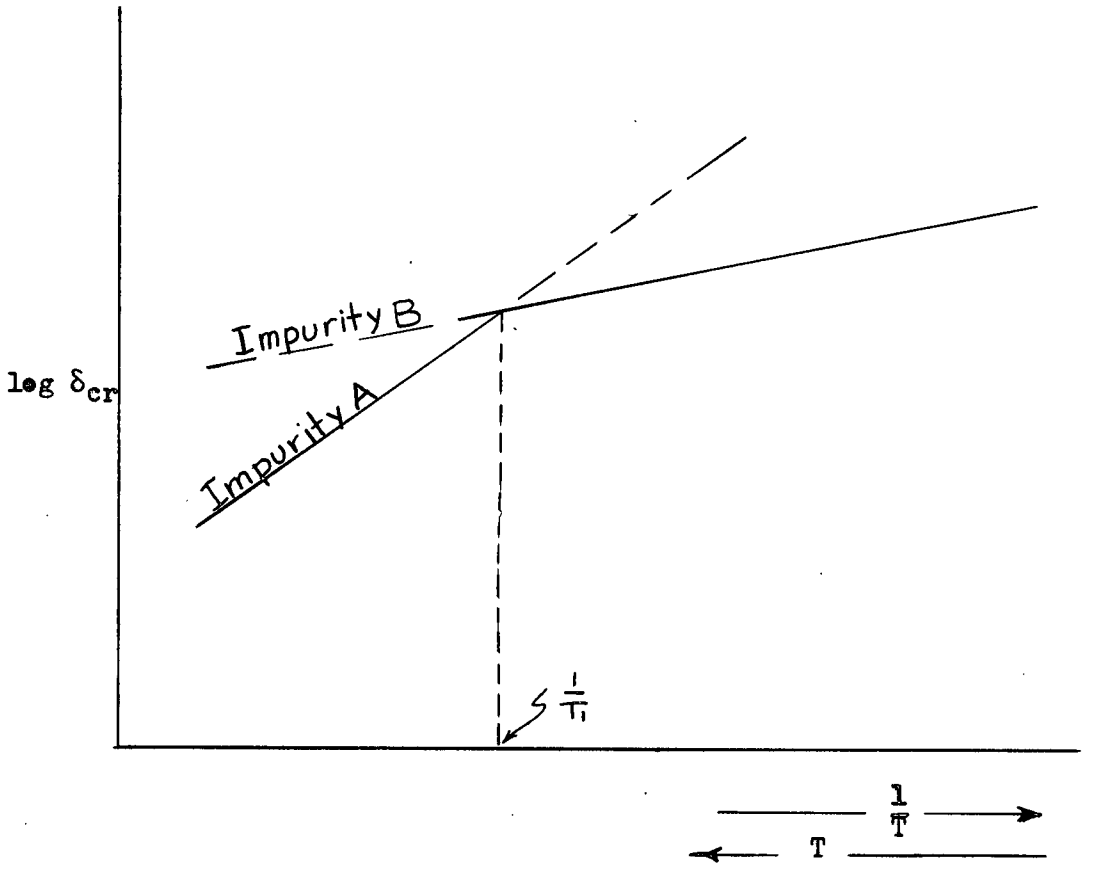

Figure 41. Hypothetical log plot of δ_{cr} VS. $1/_T$

variations in the purity of specimens tested in this region (which variations were identified) could result in higher or lower values of yield stress.

3. The percent elongation versus temperature curves (Figure 22). This curve has two regions of temperature in which ductility appears to be dropping rapidly, corresponding in each case to a rapid rise in yield stress (Figure 15). This observation is explicable in terms of the dual-impurity hypothesis, but does not fit with the ordering mechanism suggested earlier.

It is notable that the discontinuity in the temperature dependence of yield stress which was marked in the present work, was not found by other investigators working with vanadium. This may well be associated with the unusually low carbon content of the zone-refined metal employed in this study. The vanadium used by other workers contained from 4 to 20 times as much carbon, whereas the nitrogen and hydrogen contents were generally of the same order. This suggests the possibility that (referring to Figure 41) if impurity B is carbon, the curve on the log plot for carbon would be substantially higher for the vanadium used by other workers than for that used in the present study. This in turn permits the speculation that the corresponding line for another impurity (nitrogen, for example) lies below that for carbon at all temperatures down to -196°C for other investigations, but that in the present work, carbon may be the controlling impurity at temperatures below about -125°C. By way of semi-quantitative verification of this postulate, the yield stress values obtained by other workers were generally higher at the lower temperatures, but similar at the higher temperatures, relative to those obtained by the present investigator.

It should be noted that carbon and nitrogen are used as examples only in the above discussion, and that it is by no means proven that these are the dominant impurities in this mechanism.

VI. CONCLUSIONS

1. A zone-refining-melt-solidification technique for the growth of vanadium single crystals of pre-determined orientation has been perfected. Crystals 1/4-inch in diameter and up to 7 inches in length have been grown. The crystals were of more uniform cross-sectional area than those reportedly grown by workers using other metals, and the surface quality was approximately equivalent to that obtained by electropolishing.

2. Vanadium exhibits a marked temperature dependence of yield stress, as do other body-centered cubic metals. With vanadium single crystals, however, an unusual relationship between temperature and yield stress was encountered, in that a discontinuity in the plot was found between -125° and -130°C. This abnormality did not appear in nearly as pronounced a fashion on a plot of flow stress versus temperature for the metal, and therefore the anomaly is believed to be associated primarily with the initiation of yielding.

3. X-ray data proved that deformation occurred in the system $\langle 111 \rangle \{112\}$, over the whole range of temperatures studied. Therefore the discontinuity on the yield stress plot could not have been caused by a change in slip system.

4. The results of electrical resistance measurements indicated the possibility that a very minor ordering process was responsible for the anomaly, but it was considered unlikely on the basis of the magnitude of the ordering reaction.

5. The possibility of a change in deformation mechanism from slip to twinning was examined thoroughly, and, although no indisputable evidence of gross twinning was found, the mechanism is still possible. The deformation plane identified for specimens tested both above and below the

transition temperature was (112), which is also reported as the twin plane for vanadium. The coincidence of the slip and twin planes could mean that both were present in low temperature specimens, but were indistinguishable.

6. Dislocation locking due to atmospheres of more than one impurity was proposed as a possible explanation of the observed results. It depends on the formation of two impurity atmospheres around dislocation, each of which gives rise to a separate temperature dependence of yield stress. The data of another investigator[11] suggests that a similar discontinuity occurs in molybdenum, and several other metals.

7. The critical resolved shear stress on the (112) planes for a vanadium single crystal whose axial direction is [110] was found to be 11,250 psi at room temperature.

VII. RECOMMENDATIONS FOR FUTURE WORK

It is felt that a great deal might be gained by an effort to verify or reject either the dual-impurity mechanism or the deformation mechanism as described in the discussion preceding. This could be accomplished by means of controlled impurity contents and/or controlled impurity ratios in vanadium and other body-centered cubic transition metals, including iron.

A more critical study should be made of the low-temperature behaviour of other body-centered cubic refractory metals in general, both by reference to the work of previous investigators, and by experiment. Emphasis was not placed on other metals in the present work, in view of the original objectives. The recommendation would include studies of high purity polycrystalline metals and careful metallographic studies.

VIII. BIBLIOGRAPHY

1. Kinzel, A.B. - Vanadium Metal - A new Article of Commerce, Metal Progress, 58 (1950) 315.

2. Rostoker, W. - The Metallurgy of Vanadium, John Wiley and Sons, Inc., New York, (1958) 39.

3. Pugh, J.W. - Temperature Dependence of the Tensile Properties of Vanadium, Journal of Metals, 9, No. 10, Section 2, (1957) 1243-1244.

4. Tietz, T.E., Wilcox, B.A., and Wilson, J.W., Mechanical Properties and Oxidation Resistance of Certain Refractory Metals, SRI Project SU-2430, Final Report, Stanford Research Institute, 30 Jan. 59, 188.

5. Roberts, B.W. and Rogers, H.C. - Observations on Mechanical Properties of Hydrogenated Vanadium, Journal of Metals, 8, No. 10 (1956) 1213-1215.

6. Magnusson, A, and Baldwin, W.H., Jr., - Low Temperature Brittleness, Technical Report No. 34, on Contract N6onr-273/I. for office of Naval Research, March 1956.

7. Lacy, C.E., and Beck, C.J., Properties of Vanadium Consolidated by Extrusion, Transactions, A.S.M., 48, (1956), 579-594.

8. Clough, W.P. and Pavlovic, A.S. - The Flow, Fracture and Twinning of Commercially Pure Vanadium, Transactions, A.S.M., 52 Preprint 125, Aug. 1958.

9. Loomis, B.A., and Carlson, O.N., - Investigation of the Ductile-to-Brittle Transition in Vanadium, paper presented at the Reactive Metals Conference, May 27-29, 1958.

10. Farrell, J.W., - The Mechanical Properties of Unalloyed Vanadium - Technology Department Report, Union Carbide Metals Co., May 31, 1960.

11. Fisher, J.C., - Application of Cottrell's Theory of Yielding to Delayed Yield in Steel. Transactions, A.S.M., 47 (1955) 451-462.

12. Schwartzberg, F.R., Ogden, H.R., and Jaffee, R.I., Ductile-to-Brittle Transition in the Refractory Metals DMIC Report 114, Battelle Memorial Institute, 1959, 17-24.

13. Brown, C.M. - Rare Metals Handbook, Reinhold Publishing Corporation, New York, 1954, 594-596.

14. Calverly, A., Davis, M., and Lever, R.F., The Floating-Zone Melting of Refractory Metals by Electron Bombardment, Journal of Scientific Instruments, 34, (1957), 142-147.

15. Catalogue: Wheelco Instruments. Barker-Colman Co., Rockford, Ill., U.S.A., p. 5.

16. Zener, C. and Holloman, J.H., Effect of Strain Rate Upon the Plastic Flow of Steel, Journal of Applied Physics, 15, (1944) 22.

17. Holloman, J.H., and Zener, C., Conditions of Fracture in Steel, Transactions, American Institute of Mining, Metallurgical and Petroleum Engineers, 158, (1944) 283.

18. Bechtold, J.H., The effect of Temperature on the Flow and Fracture Characteristics of Molybdenum, Transactions, American Institute of Mining, Metallurgical and Petroleum Engineers, 197 (1955) 1469.

19. Bechtold, J.H., and Shewmon, P.G., Flow and Fracture Characteristics of Annealed Tungsten. Transactions, A.S.M., 47 (1955) 451.

20. Cottrell, A.H., and Bilby, B.A., Dislocation Theory of Yielding and Strain Aging in Iron, Proceedings Royal Society, London, A62 (1949) 49.

21. Steijn, R.P., and Brick, R.M., Flow and Fracture of Single Crystals of High Purity Ferrite, A.S.M. Preprint No. 36, 1953.

22. Cox, J.J., Horne, G.T. and Mehl, R.F., Slip, Twinning and Fracture in Single Crystals of Iron, Transactions, A.S.M., 49 (1956) Preprint No. 1.

23. Cullity, D.B., Elements of X-ray Diffraction, Addison-Wesley Publishing Co. Inc., Reading, Mass. (1956) 72-73.

24. Barrett, C.S., Ansel, G., and Mehl, R.F., Slip, Twinning and Cleavage in Iron and Silicon Ferrite, Transactions, A.S.M., 25 (1937) 702.

25. Fahrenhorst, N., and Schmid, E., On the Plastic Deformation of an α-Iron Crystal, Zeitschrift fur Physik, 78 (1932) 383.

26. Opinsky, A.J., and Smoluchowski, R. The Crystallographic Aspect of Slip in Body-Centered Cubic Single Crystals, Journal of Applied Physics, 22 (1951) 1488.

27. Taylor, G.I., and Elam, C.F. The Distortion of Iron Crystals, Proceedings, Royal Society, London, A112 (1926) 337.

28. Taylor, G.I., The Deformation of Crystals of B-Brass, Proceedings, Royal Society, London, A118, (1928) 1.

29. Chen, N.K., and Maddin, R., Plasticity of Molybdenum Single Crystals, Transactions, A.I.M.E., 191, (1951) 937.

30. Carlson, O.N., and Owen, C.V. Preparation of High Purity Vanadium Metal by the Iodide Refining Process, Institute for Atomic Research and Department of Chemistry, Iowa State University, Paper presented at the Electro-Chemical Society Meeting, Chicago, May 1960.

31. Adams, M.A., Roberts, A.C., and Smallman R.E., Yield and Fracture in Pollycrystalline Niobium, Acta Metallurgica, 8, No. 5 (1960) 328-337.

32. Biggs, W.D., and Pratt, P.L., α-Iron at Low Temperatures, Acta Metallurgica, 6, (1958) 694.

33. Cottrell, A.H., Dislocations and Plastic Flow in Crystals, Oxford University Press, London, 1953, 134-145.

34. Wessel, E.T., Abrupt Yielding and the Ductile-to-Brittle Transition in Body-Centered Cubic Metals, Journal of Metals, 9, No. 7 Section 2 (1957) 930-935.

IX. APPENDICES

APPENDIX I

TABLE I

THE RESULTS OF TENSILE TESTS

Specimen	Date	D initial (in)	A(10^{-2}) (in^2)	L initial (in)	L final (in)	Temp. °C	$1/T$ $^1/°K$ x10^3	% El.	P.L.(psi) (10^{-3})	UYS psi (10^{-3})	Flow Str. (10^{-3})	UTS(psi) (10^{-3})	δcr (10^{-3})psi	Remarks
V05T1	14/6/60	.119	1.111	.825	1.06	20	3.41	28.48	22.50	23.85	23.22	24.84	11.25	
V05T2	14/6/60	.120	1.130	.832	.900	-196	12.98	8.17	106.19	115.04	102.65	115.04	54.25	
V05T3	14/6/60	.137	1.474	.760	.875	-183	11.11	15.13	91.59	98.37	78.02	98.37	46.39	
V05T4	14/6/60	.134	1.410	.770	.980	20	3.41	27.27	21.99	24.45	24.11	26.24	11.53	
V04T1	2/7/60	.115	1.038	.709	.890	20	3.41	25.52	23.80	26.30	25.72	27.55	12.40	
V07T1	2/7/60	.118	1.093	.895	1.115	20	3.41	24.58	20.59	23.60	22.87	25.16	11.13	
V04T4	2/7/60	.119	1.112	.915	.947	-183	11.11	3.49	93.53	101.80	98.20	101.80	48.01	
V07T4	2/7/60	.120	1.130	.842	.923	-183	11.11	9.61	94.69	100.00	97.35	100.00	47.16	
V04T5	2/7/60	.120	1.130	.992	1.050	-196	12.98	5.84	109.29	116.81	109.73	116.81	55.09	
V07T5	2/7/60	.116	1.056	.785	.862	-196	12.98	9.80	85.23	96.78	92.80	96.78	45.64	Faulty Sp.
V08T1	26/7/60	.115	1.038	.815	1.056	24	3.37	29.57	17.82	21.39	21.00	23.70	10.09	
V08T3	26/7/60	.123	1.188	.919	1.195	24	3.37	30.03	18.52	22.73	22.14	25.08	10.72	
V08T5	26/7/60	.108	0.916	1.100	1.190	24	3.37	8.18	19.65	22.93	22.93	25.55	10.81	
V09T1	26/7/60	.116	1.056	.840	1.056	-50	4.48	25.71	28.60	33.05	32.39	34.09	15.59	
V09T3	26/7/60	.118	1.093	.825	1.036	-50	4.48	25.57	30.19	33.21	32.11	36.87	15.66	
V09T5	26/6/60	.119	1.112	.857	1.049	-50	4.48	22.40	32.82	35.07	34.53	36.15	16.54	
V04T2	27/7/60	.119	1.112	.772	.986	-50	4.48	27.72	33.09	35.70	34.08	36.33	16.84	
V07T2	27/7/60	.122	1.169	.845	1.079	-50	4.48	27.69	32.93	34.90	33.19	34.47	16.46	
V04T2	27/7/60	.122	1.169	.777	D.N.M.	-109	6.09	D.N.M	D.N.M	D.N.M	D.N.M	D.N.M	D.N.M	Faulty Sp.
V07T3	27/7/60	.120	1.130	.840	1.070	-109	6.09	27.38	46.90	53.36	51.59	53.36	25.17	
V10T1	27/7/60	.112	0.985	.807	1.090	-109	6.09	35.06	35.53	49.14	45.99	49.14	23.17	
V10T3	27/7/60	.123	1.189	.806	.962	-109	6.09	19.35	47.10	54.75	50.46	54.75	25.82	
V10T5	27/7/60	.110	0.950	.820	.987	-109	6.09	20.36	44.53	50.11	48.63	50.11	23.63	
V11T1	27/7/60	.120	1.130	.834	.995	-196	12.98	19.30	D.N.M	D.N.M	D.N.M	D.N.M	D.N.M.	Oil on grips
V11T3	27/7/60	.116	1.056	.825	.892	-196	12.98	8.12	100.38	112.69	104.17	112.69	53.15	
V11T5	27/7/60	.121	1.150	.853	.995	-196	12.98	16.64	D.N.M	D.N.M.	D.N.M	D.N.M	D.N.M	Oil on grips
V11T2	28/7/60	.113	1.003	.832	.911	-196	12.98	9.49	113.66	118.64	99.70	118.64	55.95	
V10T2	3/8/60	.104	0.849	.788	.893	-125	6.76	13.32	71.85	75.38	61.25	75.38	35.55	
V10T4	3/8/60	.122	1.169	.851	.963	-125	6.76	13.16	62.45	65.53	55.69	65.53	30.90	
V09T2	3/8/60	.120	1.130	.784	.913	-125	6.76	16.45	70.80	73.89	63.72	73.89	34.85	

V09T4	3/8/60	.114	1.020	.851	.952	-128	6.90	11.86	78.43	81.37	68.63	81.37	38.37
V12T1	4/8/60	.121	1.150	.814	.919	-140	7.52	12.33	77.39	80.09	66.43	80.09	37.77
V12T3	4/8/60	.122	1.169	.764	.882	-140	7.52	15.44	74.85	77.59	70.15	77.59	36.59
V12T4	4/8/60	.118	1.093	.802	.910	-140	7.52	13.46	78.68	81.98	65.87	81.98	38.66
V06T1	5/8/60	.114	1.020	.815	.933	-121	6.58	14.47	71.57	74.41	65.69	74.41	35.09
V12T2	5/8/60	.114	1.020	.780	.903	-121	6.58	15.76	60.78	63.73	57.84	63.73	30.06
V11T4	5/8/60	.119	1.112	.852	.995	-121	6.58	16.78	52.16	57.82	55.85	57.82	27.27
V06T2	5/8/60	.116	1.056	.798	.895	-133	7.14	12.15	73.86	76.99	70.27	76.99	36.31
V06T3	5/8/60	.1225	1.178	.848	.933	-165	9.26	10.02	86.16	89.39	86.16	89.39	42.16
V06T4	29/8/60	.117	1.075	.806	D.N.M	D.N.M	D.N.M	D.N.M.	D.N.M	D.N.M	D.N.M	D.N.M.	D.N.M Oil in grips
V06T5	29/8/60	.117	1.075	.841	D.N.M	-165	9.26	* 22	71.63	74.92	73.02	74.42	35.10 Faulty Sp.
V08T4	29/8/60	.113	1.003	.845	D.N.M	-164	9.17	* 15	85.74	88.14	78.36	88.14	41.57
V02T1	29/8/60	.1205	1.140	.800	.924	-157	8.62	15.50	77.19	81.67	74.82	81.67	38.52
V02T2	29/8/60	.110	0.950	.811	D.N.M	-128	6.90	* 18	66.32	69.16	64.11	69.16	32.62
V02T3	29/8/60	.116	1.056	.822	D.N.M	-130	6.99	* 18	67.80	71.97	62.50	71.97	33.94
V13T2	29/8/60	.1165	1.066	.868	D.N.M	-138.5	7.43	* 18	69.42	72.61	64.63	72.61	34.24
V13T3	30/8/60	.1135	1.011	.967	D.N.M	-133.5	7.17	* 18	73.18	76.58	63.91	76.58	36.12
Polycrystalline Specimens at 0.055/min.													
V15T2	30/8/60	.116	1.056	.866	D.N.M	-122.5	6.64	* 19	64.39	67.61	64.30	67.61	
V15T3	30/8/60	.1215	1.159	.833	D.N.M	-101	5.81	* 23	53.49	56.60	53.67	56.60	
V15T4	30/8/60	.120	1.130	.906	D.N.M	-62	4.74	* 24	33.98	40.27	40.27	41.59	
V16T5	30/8/60	.119	1.112	.757	.880	-136.5	7.33	16.24	69.24	73.29	69.24	73.29	
V16T3	30/8/60	.116	1.056	.760	D.N.M	-136.5	7.33	* 16	67.23	71.97	69.13	71.97	
V16T4	30/8/60	.121	1.150	.793	1.080	-159.5	9.02	36.19	88.70	93.91	86.09	93.91	
V15T5	30/8/60	.117	1.075	.882	1.057	-63	4.76	19.84	36.28	41.49	40.93	42.79	
Single Crystals at 0.0022/min.													
V14T1	31/8/60	.118	1.093	.949	1.075	-157	8.62	13.27	73.19	80.15	71.73	80.15	37.80
V14T2	31/8/60	.1205	1.140	.914	1.020	-142	7.63	11.59	71.93	74.82	59.04	74.82	35.29
V14T3	31/8/60	.116	1.056	.890	D.N.M	-137	7.35	* 10	63.45	65.25	59.19	65.25	30.77
V14T4	31/8/60	.121	1.150	.952	1.075	-134.5	7.22	12.92	65.22	66.35	54.78	66.35	31.29
V14T5	31/8/60	.1205	1.140	.971	1.079	-128	6.90	11.12	59.65	62.37	53.07	62.37	29.41

V13T4	31/8/60	.1165	1.066	.958	D.N.M	- 99.5	5.76	✱D.N.M	32.83	39.68	39.12	39.68	18.71
V13T5	31/8/60	.119	1.112	1.009	D.N.M	-132.5	7.12	✱ 10	54.86	59.35	52.16	59.35	27.99
V13T1	31/8/60	.114	1.020	.972	D.N.M	-118	6.45	✱ 11	41.18	45.69	44.12	45.69	21.55
V02T4	31/8/60	.119	1.112	.819	.890	-134.5	7.22	8.66	58.72	62.59	55.85	62.59	29.52

✱ Elongation estimated from Load-Elongation curve

AVERAGE ELONGATION DATA

	Avg. El.%
20°C	27.53
-50°C	25.81
-109°C	25.54
-121°C	15.67
-125°C	14.31
-128°C	14.93
-133.5°C	16.05
-140°C	14.80
-165°C	13.50
-183°C	9.41
-196°C	8.28

B. THE CALCULATION OF STRESS AND ELONGATION

EXAMPLE V05T1 (tested at 20°C)

STRESS

δ_y = yield stress

P = load = 264 lbs.

A = area = 1.111×10^{-2} in^2

$$\delta = P/A$$

$$= \frac{264}{1.111 \times 10^{-2}} = 23{,}850 \ \frac{lbs}{in^2}$$

ELONGATION

E = % elongation

1 in. = initial gauge length

1 f = final gauge length

$$E = \frac{1f - 1in}{1 \text{ in.}} \times 100$$

$$= \frac{1.060 - 0.825}{0.825} = 28.48\%$$

C. THE MAXIMUM ERROR IN YIELD STRESS MEASUREMENTS

EXAMPLE 1 V05T1 (tested at 20°C)

Estimated maximum error in measuring P:

$P = 264 \pm 1$ lb

$= 264 \pm 0.4\%$

Estimated maximum error in measuring A

$d = 0.119 \pm 0.0005$

$A = .7852\ (.119)^2 \pm 0.001$

$= (1.111)\ (10^{-2}) \pm .001$

$= (1.111)\ (10^{-2}) \pm 9\%$

Total maximum error in δ :

$\delta = 23{,}850 \ \frac{lb}{in^2} \pm 9.4\%$

$= 23{,}850 \pm 2220 \ \frac{lbs}{in^2}$

EXAMPLE 2 V05T2 (tested at -196°C)

Estimated maximum error in measuring P:

$$P = 1300 \pm 10 \text{ lbs.}$$

$$= 1300 \pm 0.8\ \%$$

Estimated maximum error in measuring A:

$$d = 0.120 \pm 0.0005 \text{ in.}$$

$$A = .7852\ (0.120)^2 \pm 0.001$$

$$= 1.130 \times 10^{-2} \pm 0.001$$

$$= 1.130 \times 10^{-2} \pm 8.9\%$$

Total maximum error in δ :

$$\delta = P/A = \frac{1300 \pm 0.8}{1.130 \times 10^{-2} \pm 8.9}$$

$$= 115{,}040 \pm 9.7\%$$

$$= 115{,}040 \pm 11{,}160 \ \frac{\text{lbs}}{\text{in}^2}$$

It should be remembered the values stated are maximum values, and in nearly all cases, the accuracy would be much better.

D. THE PROBABLE ERROR IN YIELD STRESS MEASUREMENTS

EXAMPLE V05T1

$$P = 264 \pm 1$$

$$= 264 \pm 0.4\%$$

$$A = .7852\ (.119)^2 \pm .0002$$

$$= 1.111 \times 10^{-2} \pm 1.8\%$$

Probable error in δ

$$\delta = \frac{264 \pm 0.4\%}{(1.111)(10^{-2}) \pm 1.8\%}$$

$$= 23850 \pm 2.2\% = 23850 \pm 525 \text{ psi.}$$

EXAMPLE 2 V05T2

$P = 1300 \pm 10$ lbs

$= 1300 \pm 0.8\ \%$

$A = (.7852)(0.120)^2 \pm 0.0002$

$= 1.130 \times 10^{-2} \pm 1.77\%$

Probable error in δ :

$$\delta = \frac{1300 \pm .8\%}{(1.130)(10^{-2}) \pm 1.77} = 115{,}040 \pm 2.57\%$$

$\delta = 115{,}040 \pm 2960$ psi

E. CALCULATION OF CRITICAL RESOLVED SHEAR STRESS

$$\delta cr = P/_A \cos \phi \cos \lambda$$

ϕ = Angle between perpendicular to slip plane and tension axis

λ = Angle between [111] and tension axis

P = load

A = area

$P/_A$ = yield stress = δ_y

EXAMPLE V05T1 (tested at room temperature)

$\delta_y = 23{,}850$ psi.

$= 35°18'$

$= 54°42'$

$\cos \lambda = 0.81614$

$\cos \phi = 0.57786$

$\delta cr = 23{,}850\ (0.81614)\ (0.57786)$

$= 11{,}250$ psi.

APPENDIX II

The Zone Refiner

A. ELECTRICAL SYSTEM

Figure 1 shows the circuit diagram for the zone refiner. It closely resembles the one designed by Calverley, Davis and Lever[14], and uses the same current control system, that is by emission control, in which the filament temperature controls the emission current.

Modification to Power Supply

There are a number of ways in which a power system of the type used in this work could be greatly improved. The first and most important is in the current stabilization. The present system contains a time lag which arises from the time it takes for the filament to change temperature. The modification suggested by Calverly, Davis and Lever[14], is to supply the high voltage from a constant current source. In this system, the bombardment current is kept constant by adjusting the high voltage.

A number of minor improvements which could be made are: the use of very high speed relays to shut off the high voltage when a short circuit occurs, the use of smaller and more compact transformers, both to decrease the weight and increase the efficiency of operation, the use of a single thyratron tube in the control circuit, since it was found in the present work that only one of them operated at any one time. However they were found to alternate, and in changing, they often caused the high voltage to cut out, resulting in annoying delays.

B. FURNACE SYSTEM

It is felt by the author that the existing design of the furnace part of the zone refiner is unsatisfactory and should be rebuilt in the manner described below. Rather than have 2 brass plates suspended by a

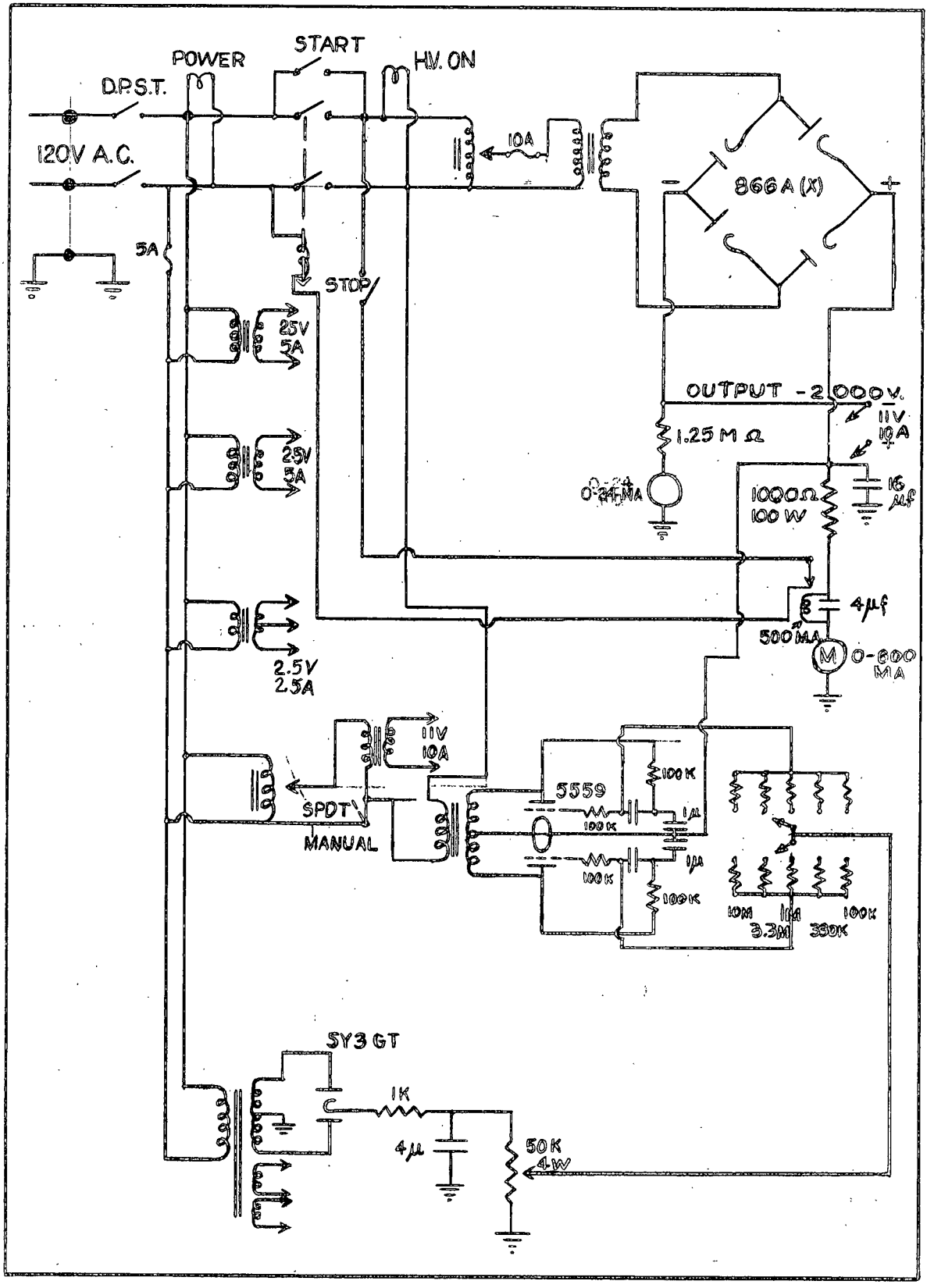

Figure 1. Circuit Diagram of the Zone Refiner as used in this investigation.

large pyrex tube as was the case in the present work, the whole assembly should be mounted on one plate which serves as the base and leads to the vacuum system. A bell jar should be used for the vacuum chamber. This would greatly facilitate working around and on the apparatus. The drive should consist of a down-driven worm gear. This is useful for two reasons: (1) a zone which moved upwards (i.e. the specimen moves down) would provide a more stable zone, and (2) a worm gear drive would provide a much more uniform movement.

It is felt that the present system of specimen mounting, filament type, beam-focus plates and radiation shields are satisfactory except that it would be convenient to have a reflected view of the molten zone, since metals with high vapor pressures very quickly deposit a layer of vaporized metal onto the viewing glass, thus obscuring the zone.

APPENDIX III

RESISTANCE MEASUREMENTS

TABLE I

THE RESULTS OF RESISTANCE MEASUREMENTS

Vernier μ volts (pot.)	Potentiometer μ Volts (Current)	I (amps)	R (μ ohms)	T (°K)	Remarks
116.7	7877.3	.78773	148.1	126.0	Run 1
130.0	7916.9	.79169	164.2	136.0	No Load
140.6	7785.5	.77855	180.6	145.0	
151.0	7794.7	.77947	193.7	150.0	
161.7	7952.0	.79520	203.3	158.5	
171.2	7816.9	.78169	219.0	166.0	
181.0	7891.3	.78913	229.4	173.5	
190.3	7820.8	.78208	243.3	185.5	
195.4	7733.1	.77331	252.7	189.0	
200.0	7492.8	.74928	266.9	197.0	
213.8	7573.9	.75739	282.3	206.0	
233.8	7773.2	.77732	300.8	216.0	
252.5	7772.1	.77721	324.9	229.0	
281.2	7794.4	.77944	360.8	250.5	
300.0	6960.0	.69600	431.0	269.5	
57.5	8050.1	.80501	71.4	75.5*	Run 2
64.1	8944.6	.89446	71.7	75.5	Load = 40,000
78.5	8963.3	.89633	87.6	87.0	psi.
93.7	8980.2	.89802	104.3	97.0	* No load
108.1	8977.2	.89772	120.4	111.0	
114.3	8974.9	.89749	127.4	112.0	
131.0	8972.4	.89724	146.0	121.0	
137.0	8974.6	.89746	152.7	126.5	
146.8	8968.2	.89682	163.7	131.5	
154.4	8965.6	.89656	172.2	137.0	
161.5	8965.3	.89653	180.1	141.0	
168.7	8965.6	.89656	188.2	146.0	
174.1	8965.6	.89656	194.2	150.0	
176.6	8966.9	.89669	196.9	152.0	
184.6	8966.7	.89667	205.9	156.5	
193.2	8967.2	.89672	215.5	160.0	
206.3	8964.4	.89644	230.1	168.0	
213.4	8964.3	.89643	238.1	172.0	
220.9	8967.4	.89674	246.3	174.5	

Vernier μ volts (psi)	Potentiometer μ volts (Current)	I (amps)	R (μ ohms)	Stress(psi)	Remarks
51.4	7074.5	.70745	72.7	0	Run 3
54.0	7374.2	.73742	73.2	10,000	No lead to
48.8	6600.0	.66000	73.9	20,000	yield stress
118.8	16059.2	1.60592	74.0	30,000	at constant
119.6	16154.9	1.61549	74.0	40,000	temperature
117.4	15726.7	1.57267	74.7	50,000	(liquid N_2 =
120.6	16207.7	1,62077	74.4	60,000	-196°C)
121.2	16227.7	1.62277	74.7	70,000	
121.4	16236.5	1,62365	74.8	80,000	
121.4	16239.3	1.62393	74.8	90,000	
122.1	16173.6	1.61736	75.5	100,000	
				T(°K)	
116.1	15734.4	.157344	73.8	75.0	Run 4
127.6	15665.6	.156656	81.5	83.0	lead =
142.0	15660.8	.156608	90.7	88.0	70,000 psi
162.5	15632.0	.156320	104.0	99.5	
196.9	15688.7	.156887	125.5	111.0	
56.0	7761.6	.77616	72.2	78.5	Run 5
74.0	7400.0	.74000	100.0	93.0	No lead
76.9	7215.5	.72155	106.6	100.0	(Repeat)
85.9	7258.0	.72580	118.4	106.0	
93.1	7443.2	.74432	125.1	113.0	
102.6	7403.7	.74037	138.6	119.5	
106.0	7130.0	.71300	148.7	126.0	
114.5	7186.7	.71867	159.3	130.5	
124.4	7224.2	.72242	172.2	139.5	
139.9	7183.8	.71838	194.7	150.5	
147.9	7176.9	.71769	206.1	159.0	
160.8	7225.8	.72258	222.5	166.5	
179.2	7330.0	.73300	244.5	177.0	
185.2	7259.8	.72598	255.1	183.0	
186.9	6926.2	.69262	268.5	194.0	
194.8	6925.9	.69259	281.3	198.5	
203.0	6924.0	.69240	293.2	204.5	
216.6	7103.7	.71037	304.9	215.0	
237.5	7279.8	.72798	326.2	227.0	
260.0	7569.9	.75699	343.5	238.0	
278.8	7663.5	.76635	363.8	251.0	
291.5	7641.5	.76415	381.5	263.0	
298.3	7334.3	.73393	406.4	274.0	

B. CALCULATION OF ELECTRICAL RESISTANCE

The resistance measurements were set up such that one set of leads measured the current passing through the specimen and a standard resistance of 0.01 ohm, while the other set of leads measured the potential.

μV_p = potential voltage (micro-volts)

μV_c = current voltagee (micro-volts)

I = current in amps

R = resistance in micro ohms

SAMPLE CALCULATION

μV_p (measured) = 116.7 μ volts

μV_c (measured) = 7877.3 μ volts

$$I = \frac{7877.3}{0.01} \times 10^{-6} = 0.78773 \text{ amps}$$

$$R = \frac{116.7}{0.78773} = 126.0 \text{ micro-ohms}$$

C. CALCULATION OF MAXIMUM ERROR IN RESISTANCE MEASUREMENTS

$$R = \frac{\mu V_p}{I}$$

Maximum % Error in R = % error in μV_p + % error in I.

Maximum % error in I = % error in μV_c + % error in R

≈ 0

Maximum % error in μV_c = 0.2% (estimated)

Maximum % error in R $\pm$ 0.2%

at a temperature of 150°K

R is approximately 150 μ ohms.

Therefore Error in R = $\pm$ 0.3 μ ohms

% error in temperature[15] at 150°K is $\pm$ 2%

Therefore error in T = $\pm$ 3°K

These error values are probably much too large, since the error in temperature measurement is compensating.

APPENDIX IV

MICROHARDNESS

TABLE I

THE RESULTS OF MICROHARDNESS MEASUREMENTS

$KHN = 14.229 \; L/l^2$

L = lead (kgms)

l = length of indentation (mm)

★ Values taken from Departmental Tables

Specimen	Avg. Filar Units	Length(mm)	KHN	Remarks
V02T3	775.3	0.368	105.1	
V04T3	738.4	0.351	115.5	
V05T3	775.0	0.368	105.1	
V06T3	733.2	0.348	117.5	
V07T3	691.3	0.328	132.3 ★	
V08T3	735.2	0.349	116.8 ★	
V09T3	664.0	0.315	143.4 ★	
V10T3	784.5	0.373	102.3	
V11T3	784.6	0.373	102.3	
V12T3	756.6	0.359	110.4	
V13T3	815.3	0.387	95.01	
V14T3	773.7	0.368	105.1	
V15T3	676.0	0.321	138.1	polycrystalline
V16T3	685.4	0.326	133.9	polycrystalline
As Received	687.1	0.326	133.9	polycrystalline

★ Results invalid because of extensive deformation which specimens underwent.